Anomalies in the equilibrium and nonequilibrium properties of correlated ions in complex molecular environments

Sathiya Mahakrishnan, Subrata Chakraborty, and Amrendra Vijay*
Department of Chemistry, Indian Institute of Technology Madras, Chennai 600036, India
(Received 28 May 2017; revised manuscript received 21 August 2017; published 22 November 2017)

Emergent statistical attributes, and therefore the equations of state, of an assembly of interacting charge carriers embedded within a complex molecular environment frequently exhibit a variety of anomalies, particularly in the high-density (equivalently, the concentration) regime, which are not well understood, because they do not fall under the low-concentration phenomenologies of Debye-Hückel-Onsager and Poisson-Nernst-Planck, including their variants. To go beyond, we here use physical concepts and mathematical tools from quantum scattering theory, transport theory with the *Stosszahlansatz* of Boltzmann, and classical electrodynamics (Lorentz gauge) and obtain analytical expressions both for the average and the frequency-wave vector-dependent longitudinal and transverse current densities, diffusion coefficient, and the charge density, and therefore the analytical expressions for (a) the chemical potential, activity coefficient, and the equivalent conductivity for strong electrolytes and (b) the current-voltage characteristics for ion-transport processes in complex molecular environments. Using a method analogous to the notion of Debye length and thence the electrical double layer, we here identify a pair of characteristic length scales (longitudinal and the transverse), which, being wave vector and frequency dependent, manifestly exhibit nontrivial fluctuations in space-time. As a unifying theme, we advance a quantity (inverse length dimension), $g^{(a)}_{\rm scat}$, which embodies all dynamical interactions, through various quantum scattering lengths, relevant to molecular species a, and the analytical behavior which helps us to rationalize the properties of strong electrolytes, including anomalies, in all concentration regimes. As an example, the behavior of $g^{(a)}_{\rm scat}$ in the high-concentration regime explains the anomalous increase of the Debye length with concentration, as seen in a recent experiment on electrolyte solutions. We also put forth an extension of the standard diffusion equation, which manifestly incorporates the effects arising from the underlying microscopic collisions among constituent molecular species. Furthermore, we show a nontrivial connection between the current-voltage characteristics of electrolyte solutions and the Landauer's approach to electrical conduction in mesoscopic solids and thereby establish a definite conceptual bridge between the two disjoint subjects. For numerical insight, we present results on the aqueous solution of KCl as an example of strong electrolyte, and the transport (conduction as well as diffusion) of K^+ ions in water, as an example of ion transport across the voltage-gated channels in biological cells.

DOI: 10.1103/PhysRevE.96.052133

I. INTRODUCTION

Microscopic dynamics of interacting charged molecular species in the presence of external electromagnetic fields or the fields originating from electrically polarizable medium (embedding solvent, for example) manifest in a variety of nontrivial emergent equilibrium and nonequilibrium statistical phenomena in electrochemical, soft matter, and biophysical systems [1], representative examples of which include (a) the physical chemistry of strong electrolytes and electrically charged interfaces [2], (b) selective transport of molecular ions in nanofluidic systems such as the naturally occurring transmembrane protein channels within the crowded environment of biological cells [3–8], (c) the transport of charged carriers in mesoscopic semiconductors such as the photovoltaic cells and nanometer-sized molecular devices [9], and so forth. To develop unambiguous conceptual understanding, predictive mathematical frameworks and practical computational protocols for such diverse varieties of complex molecular systems are some of the major intellectual challenges of physical science today. There is a rich history associated with this subject, which spans a century of scientific efforts and includes the pioneering analytical works in physical chemistry of Debye, Hückel, Falkenhagen, Onsager, Fuoss, Nernst, Planck, Mayer, Kirkwood, and others [10–24] and the equally relevant theoretical works on electrical conduction in hard condensed matter and mesoscopic systems of Drude, Sommerfeld, Bloch, Landau, Kubo, Kohn, Luttinger, Landauer, and others [25–35]. Still, the present state of affairs on our understanding of interacting ensembles of charged carriers in complex molecular environment, as we briefly review the chemical physics context below, is not completely satisfactory. The central objective of the present work is to advance an *ab initio* theoretical framework, which unambiguously bridges the microscopic world of molecules with the statistical nature of emergent phenomena, to study a variety of equilibrium as well as nonequilibrium properties of systems consisting of correlated charge carriers, which are embedded within a complex molecular environment such as the solvent or biological cells, in the presence of external electromagnetic fields.

Let us consider, as an example, the case of strong electrolytes, for which the chemical potential (and therefore the activity coefficient, γ) and the equivalent conductivity, Λ, for the electrolyte in a given solvent atmosphere serve as convenient physical observables [2]. Experimentally, in the regime of low concentrations, $\ln\gamma$ and Λ both are known to decrease

*avijay@iitm.ac.in

as one increases the concentration, $\langle n \rangle$, of the electrolyte. This behavior of strong electrolytes famously falls within the framework of Debye-Hückel-Onsager (DHO) phenomenology and is well understood [2,10–20]. In the high-concentration regime, on the other hand, both $\ln \gamma$ versus $\langle n \rangle$ and Λ versus $\langle n \rangle$ curves exhibit a variety of nontrivial anomalies ($\ln \gamma$ and Λ may increase as we increase $\langle n \rangle$, for example), which are beyond the predictions of the original DHO phenomenology and for which we do not yet possess a completely satisfactory microscopic understanding, even though there have been important advances within the framework of the Ornstein-Zernike equation and the hypernetted-chain-closure protocol [36]. To rationalize experimental observations in the high-concentration regime, there have been a number of theoretical studies [2,37–72], which, while retaining the key elements of the DHO phenomenology, introduce a number of additional adjustable parameters to improve upon the original DHO predictions on strong electrolytes, with varying degrees of success. Notable recent studies are based on the framework of time correlation functions [67–70]. These advances, though useful, are mostly executed from within the DHO framework and hence they are, in essence, tentative in character. In fact, the dynamical properties of strong electrolytes and associated ions in the high-concentration regime remains a subject of lively debate today, particularly in the biological setting [7,8]. Why is the DHO formalism or its variants not so successful in the high-concentration regime? To decipher the possible reasons, we here highlight two important conceptual shortcomings associated with the DHO paradigm and its various extensions. First, it is based on classical electrostatics [46,73]; that is, the influence of the vector potential and the dynamical aspect of the scalar potential are simply absent. This has important consequences. As an example, the use of frequency-dependent 4-potentials, as the present work reveals, necessarily introduces two distinct frequency- and wave-vector-dependent length scales: (a) the *longitudinal* one, which is analogous to but conceptually transcends the notion of *Debye length,* and (b) the *transverse* length, which is nonzero only at finite frequencies and therefore is completely absent in DHO-based phenomenologies. The spatial and frequency dispersions imply that these length scales would potentially exhibit nontrivial fluctuations in space-time, leading to interesting but yet unexplored emergent phenomena involving correlated ions in electrolyte solutions and biophysical contexts. Next, the DHO framework does not explicitly take congnizance of the inertial mass of charge carriers, constituting the electrolyte; that is, the atomic and molecular masses of various charge carriers are not manifestly present in various DHO-based mathematical expressions for chemical potentials, activity coefficients, and equivalent conductivities. That means a DHO-based theory of strong electrolytes would not manifestly differentiate, for example, a Na^+ ion from a K^+ or $(NH_4)^+$ ion, thus defeating the very purpose of chemical and inertial identities for ions in molecular science. Next, we consider the question of selective ion transport in transmembrane channels and pumps within the crowded atmosphere of biological cells [3–5]. To understand the physical mechanism of ion flow across the cell membrane, one frequently uses concepts emanating from the DHO phenomenology and employs the framework of the Nernst-Planck equation [17–20] along with the Poisson equation to model the electrostatic interactions among various charged molecular species [44–57]. The resulting Poisson-Nernst-Planck (PNP) framework and its variants do capture important aspects of the chemical physics of ion flow, but they also miss, like DHO and its variants, key conceptual elements due to the absence of the dynamical aspects of the electromagnetic potentials in the theory. Also, like DHO, the PNP phenomenology does not manifestly take the inertial mass of the charged molecular species into consideration. An objective of the present work is to develop a theoretical formalism that does not suffer from these shortcomings.

The key question now is as follows: What is a conceptually rigorous as well as practically feasible theoretical paradigm to study the nonequilibrium properties of the ensemble of charge carriers, embedded within a complex molecular environment, in the presence of the external electromagnetic fields, in a faithful manner? The equilibrium properties would be obtained simply as the space-time average of the corresponding nonequilibrium expressions. To this end, we here use the framework of the Boltzmann transport equation (BTE), for it provides a practical and unifying basis to unambiguously rationalize a wide variety of nonequilibrium statistical phenomena in terms of the fundamental scattering events taking place within the microscopic world of molecules [74–76]. This point of view for an assembly of correlated ions has a close parallel with the Fermi liquid theory program of Landau and others [30,31,77,78], which have found wide usage in the theory of metals [79]. This approach is also conceptually consistent with the viewpoint that the dynamics of microscopic collisions eventually provides a mechanism for the many-body systems to approach the state of statistical equilibrium [80]. Other theoretical approaches based on the notion of stochasticity, such as the Fokker-Planck-type equations, are useful, but they are essentially approximate implementations of the BTE [81]. In the present work, therefore, we use the following set of coupled Boltzmann-Maxwell equations in the Lorentz gauge to study the nonequilibrium properties of correlated charged molecular species in the presence of external electromagnetic fields:

$$\sum_{\mu} \partial_\mu A^\mu = 0 \quad \text{and} \quad \sum_{\nu} \partial_\nu \partial^\nu A^\mu = \frac{1}{\epsilon_0 c^2} j^\mu \quad \left(\text{with} \partial_\mu = \left\{ \frac{1}{c}\frac{\partial}{\partial t}, \vec{\nabla} \right\} \right), \tag{1}$$

$$\left(\frac{\partial}{\partial t} + \sum_i [\eta_i, \hat{H}_{\text{eff}}] \frac{\partial}{\partial \eta_i} - \sum_{\text{b}} \hat{G}_{\text{ab}} \right) f_a(\vec{r}, \vec{k}, t) = 0. \tag{2}$$

In Eq. (1), A^μ and j^μ are the 4-vectors associated with the potentials and the currents respectively. In Eq. (2), (η_1, η_2, η_3) and (η_4, η_5, η_6) respectively are the components of the position $\vec{r}$ and the wave vector $\vec{k}$ of molecular species a. $\hat{H}_{\text{eff}}$ is the effective one-particle Hamiltonian including the external fields, the symbol $[\cdots]$ stands for the Poisson bracket, and the quantity $\sum_b \hat{G}_{\text{ab}}$ denotes the collision operator which formally accounts for the absorption and emission of molecular species a from a definite wave-vector range due to scattering. We here obtain an analytical solution for Eqs. (1) and (2) and then derive analytically closed-form expressions for the charge density, current densities, equivalent conductivities, diffusion

coefficient, chemical potential, activity coefficient, and the current-voltage curves. Furthermore, we advance a quantity, designated as the *intrinsic wave vector* of magnitude $g^{(a)}_{scat}$, which is of inverse length dimension, to be a fundamental attribute (like the effective mass and the effective charge) of the molecular species a, in a given complex molecular environment. This quantity embodies all dynamical interactions present in the system and helps us to faithfully rationalize various equilibrium and nonequilibrium properties of the ensemble of correlated ions. To be specific, $g^{(a)}_{scat}$, in general, depends on the temperature, external potentials, and the concentration (equivalently, the density) of molecular species present in the system. The detailed mathematical nature of the fluctuations in $g^{(a)}_{scat}$ is, *inter alia*, the fundamental key here that (a) reveals the rich variety of physical scenarios, which the molecular systems of chemical and biophysical interests may potentially exhibit in various experiments, and (b) allows us to transcend the predictions of DHO-type phenomenology. As an example, the concentration dependence of $g^{(a)}_{scat}$ explains a recent experimental observation on NaCl in water and an ionic liquid solution at high concentrations, wherein the Debye length, beyond a certain electrolyte concentration, anomalously increases as the concentration increases [82]. Notably, the present work rests on the ideas of classical mechanics, except on two fronts. First, we use the formalism of quantum scattering theory [83–85], to obtain an expression for the collision operator, $\hat{G}_{ab}$, to be used in Eq. (2). Next, we normalize the distribution function, $f_a(\vec{r},\vec{k},t)$ in Eq. (2), in the dimensionless phase space, which is spanned by the position, $\vec{r}$, and the wave vector, $\vec{k}$, of the molecular species under consideration. Given that $\hbar\vec{k}$ stands for the linear momentum, this essentially means that the classical phase space, spanned by the position and the linear momentum of point particles, has been coarse grained over the dimension of $\hbar^3$ ($\hbar = h/2\pi$ and h is the Planck constant), which effectively takes care of the Gibbs paradox of classical statistical mechanics. Finally, we here use the following convention for the Fourier transformation: $(2\pi)^2 f(\vec{r},t) = \iint d^3g d\omega f(\vec{g},\omega)\exp[i(\vec{g}\cdot\vec{r} - \omega t)]$.

The paper is organized as follows. In Sec. II, we define the necessary constitutive relations that connect, in the Fourier $(\vec{g},\omega)$ space, the longitudinal and transverse conduction current densities with the external electric fields and the diffusion current density with the concentration (equivalently, the number density) gradient in the system. In Sec. III, we present a brief summary of classical microscopic electrodynamics in the Lorentz gauge and present various expressions, connecting the electromagnetic fields and potentials with the charge and current densities, used here. In Sec. IV, we use a simple expression for the collision operator to solve the Boltzmann transport equation in the Fourier $(\vec{g},\omega)$ space and obtain an analytical expression for the nonequilibrium distribution function, which we use in Sec. V to derive expressions for the fundamental set of observables, such as the nonequilibrium charge density and transverse-longitudinal current density. In Sec. V, we also obtain analytical expressions for the average and the frequency- and wave-vector-dependent longitudinal and transverse conductivities and the coefficient of diffusion. In Sec. VI, we present a relation between the longitudinal current density and the charge density, which reveals the role of molecular collisions in providing a mechanism for dissipation, which, in turn, suggests a new effective equation of motion for diffusive transport that manifestly incorporates the influence of microscopic scattering events among constituent molecular species. In Sec. VII, we advance a physical meaning to the infinite self-energy and obtain a renormalized expression for the singularity-free longitudinal electric field, useful for computing observables. In Sec. VIII A, we use the Poynting theorem [86] to obtain an analytical expression for the chemical potential. In Secs. VIII B and C, we compute the activity coefficient and equivalent and molar conductivity for z:z-valent binary electrolytes, discuss their behavior in the low- as well as high-concentration regimes, and contrast them with the original DHO phenomenology. In Sec. VIII D, we obtain an expression for the current-voltage curves, useful for understanding ion-transport processes in biological channels and pumps. In Sec. VIII D, we also show a nontrivial connection between the present expression for the current-voltage curve and the Landauer's approach to electron conduction in mesoscopic systems [32–34] and thereby establish a conceptual bridge between the two apparently disjoint fields of research. In Sec. VIII E, we discuss the behavior of the coefficient of diffusion as a function of the concentration of diffusing molecules, which is useful to rationalize the phenomenon of anomalous diffusion, frequently encountered in physical and biological sciences. We conclude the paper with a brief outline on future outlook in Sec. IX.

II. CONSTITUTIVE RELATIONS

Basic observables of interest here are the current density, arising either due to the concentration (equivalently, the density) gradient (diffusion current, $\vec{J}^{(diff)}_{||}$) or due to the external electromagnetic fields (longitudinal, $\vec{J}^{(drift)}_{||}$, and the transverse conduction current, $\vec{J}^{(drift)}_{\perp}$) or both. We therefore introduce relevant constitutive relations, in the Fourier $(\vec{g},\omega)$ space, as follows:

$$\vec{J}^{(drift)}_{||}(\vec{g},\omega) = \sigma_{||}(\vec{g},\omega)\vec{E}_{||}(\vec{g},\omega), \tag{3}$$

$$\vec{J}^{(drift)}_{\perp}(\vec{g},\omega) = \sigma_{\perp}(\vec{g},\omega)\vec{E}_{\perp}(\vec{g},\omega), \tag{4}$$

$$\vec{J}^{(diff)}_{||}(\vec{g},\omega) = -igD_{||}(\vec{g},\omega)n(\vec{g},\omega)\hat{g}, \tag{5}$$

where $\vec{E}_{||}(\vec{g},\omega) = [\hat{g}\cdot\vec{E}(\vec{g},\omega)]\hat{g}$ and $\vec{E}_{\perp}(\vec{g},\omega) = \vec{E}(\vec{g},\omega) - \vec{E}_{||}(\vec{g},\omega)$ respectively are the longitudinal and transverse components of the electric field. In the orthogonal coordinate system defined by the set, $\{\hat{e}_i, i = 1,2,3\}$, of unit vectors, we have $\vec{g} = \sum_{i=1}^{3} g_i\hat{e}_i$ and therefore $\vec{E}_{||}(\vec{g},\omega)$ and $\vec{E}_{\perp}(\vec{g},\omega)$ have the following representations:

$$\vec{E}_{||}(\vec{g},\omega) = \sum_{j=1}^{3}\left[\sum_{i=1}^{3}\left(\frac{g_i g_j}{g^2}\right)E_i(\vec{g},\omega)\right]\hat{e}_j, \tag{6}$$

$$\vec{E}_{\perp}(\vec{g},\omega) = \sum_{j=1}^{3}\left[\sum_{i=1}^{3}\left(\delta_{ij} - \frac{g_i g_j}{g^2}\right)E_i(\vec{g},\omega)\right]\hat{e}_j. \tag{7}$$

The quantity $D_{||}(\vec{g},\omega)$, in Eq. (5), is the coefficient of diffusion and $n(\vec{g},\omega)$ represents the number density of the molecular

species. In Eqs. (3) and (4), $\sigma_{\parallel}(\vec{g},\omega)$ and $\sigma_{\perp}(\vec{g},\omega)$ respectively stand for the longitudinal and transverse conductivities. With Eqs. (3)–(5), the expression for the total current density takes the following form:

$$\hat{e}_{\rm j}\cdot\vec{J}(\vec{g},\omega)=\sum_{\rm l=1}^{3}\sigma_{\rm jl}(\vec{g},\omega)E_{\rm l}(\vec{g},\omega)-ig_{\rm j}D_{\parallel}(\vec{g},\omega)n(\vec{g},\omega), \tag{8}$$

$$\text{where } \sigma_{\rm jl}(\vec{g},\omega)=\delta_{\rm jl}\sigma_{\perp}(\vec{g},\omega)+\frac{g_{\rm j}g_{\rm l}}{g^2}[\sigma_{\parallel}(\vec{g},\omega)-\sigma_{\perp}(\vec{g},\omega)] \tag{9}$$

$$\begin{aligned}\Rightarrow\ &\vec{J}(\vec{r},t)\\ &=\sum_{\rm j=1}^{3}\hat{x}_{\rm j}\Bigg[\frac{1}{2\pi^2}\int_{-\infty}^{\infty}\int_{-\infty}^{\infty}d^3r'dt'h(t-t')\\ &\quad\times\Bigg\{\Bigg[\sum_{\rm l=1}^{3}\sigma_{\rm jl}\left(\frac{\vec{r}}{2}-\vec{r}',t-t'\right)E_{\rm l}\left(\frac{\vec{r}}{2}+\vec{r}',t'\right)\Bigg]\\ &\quad-\Bigg[D_{\parallel}\left(\frac{\vec{r}}{2}-\vec{r}',t-t'\right)\Bigg[\frac{\partial}{\partial x_{\rm j}''}n(\vec{r''},t')\Bigg]_{\vec{r''}=\frac{\vec{r}}{2}+\vec{r}'}\Bigg]\Bigg\}\Bigg],\end{aligned} \tag{10}$$

where the Heaviside step function, $h(t-t')$, accounts for the causality in the time domain.

III. ELECTROMAGNETIC POTENTIALS

Necessary relations among the charge and current densities and the electromagnetic potentials and the fields used in the present study are derived from Eq. (1), which, in the Cartesian $(\vec{g},\omega)$ space, yields the following set of equations for the scalar, $\phi(\vec{g},\omega)$, and the vector potential, $\vec{A}(\vec{g},\omega)$, and thence the electric, $\vec{E}(\vec{g},\omega)$, and magnetic field, $\vec{B}(\vec{g},\omega)$ [86]:

$$\vec{A}(\vec{g},\omega)=\frac{\mu}{g^2-\mu\epsilon\omega^2}\vec{J}(\vec{g},\omega), \tag{11}$$

$$\phi(\vec{g},\omega)=\frac{1}{\epsilon\left(g^2-\mu\epsilon\omega^2\right)}\rho(\vec{g},\omega), \tag{12}$$

$$\vec{A}_{\parallel}(\vec{g},\omega)=\frac{\omega\mu\epsilon}{g}\phi(\vec{g},\omega)\hat{g}, \tag{13}$$

$$\vec{B}(\vec{g},\omega)=i\vec{g}\times\vec{A}_{\perp}(\vec{g},\omega), \tag{14}$$

$$\vec{E}(\vec{g},\omega)=i[\omega\vec{A}(\vec{g},\omega)-\vec{g}\phi(\vec{g},\omega)], \tag{15}$$

where $\rho(\vec{g},\omega)$ is the charge density. Notably, the potentials in Eqs. (11) and (12) and the gauge in Eq. (13) imply the conservation of free charges, as shown below:

$$\vec{J}_{\parallel}(\vec{g},\omega)=\frac{\omega}{g}\rho(\vec{g},\omega)\hat{g}. \tag{16}$$

Finally, from Eqs. (11)–(16), we have the following expressions for the electric and magnetic fields in the Fourier $(\vec{g},\omega)$ space:

$$\begin{aligned}\vec{E}_{\parallel}(\vec{g},\omega)&=i[\omega\vec{A}_{\parallel}(\vec{g},\omega)-\vec{g}\phi(\vec{g},\omega)]\\ &=\frac{i\hat{g}}{g}(\mu\epsilon\omega^2-g^2)\phi(\vec{g},\omega)\\ &=-\frac{i}{g\epsilon}\hat{g}\rho(\vec{g},\omega)=-\frac{i}{\omega\epsilon}\vec{J}_{\parallel}(\vec{g},\omega),\end{aligned} \tag{17}$$

$$\vec{E}_{\perp}(\vec{g},\omega)=i\omega\vec{A}_{\perp}(\vec{g},\omega)=\frac{i\omega\mu}{g^2-\mu\epsilon\omega^2}\vec{J}^{f}_{\perp}(\vec{g},\omega), \tag{18}$$

$$\vec{B}_{\perp}(\vec{g},\omega)=\frac{ig\mu}{g^2-\mu\epsilon\omega^2}\hat{g}\times\vec{J}_{\perp}(\vec{g},\omega). \tag{19}$$

That is, it is the finite values of the wave vector, $\vec{g}$, that differentiate the notion of the transverse vector field, $\vec{E}_{\perp}(\vec{g}=0,\omega)$, from the longitudinal one, $\vec{E}_{\parallel}(\vec{g}=0,\omega)$, as Eqs. (17) and (18) reveal.

IV. BOLTZMANN EQUATION

We here use the BTE as given in Eq. (2) and outline a controlled sequence of approximations to obtain an expression for the nonequilibrium distribution function, useful for computing a variety of molecular observables. For charged molecular species of type a in the presence of external electromagnetic fields, Eq. (2) reads as follows [75]:

$$\begin{aligned}&\left[\frac{\partial}{\partial t}+\frac{\hbar}{m_{\rm a}}\vec{k}\cdot\vec{\nabla}_r+\frac{1}{\hbar}\vec{F}^{\rm (a)}(\vec{r},t)\cdot\vec{\nabla}_k\right]f_{\rm a}(\vec{r},\vec{k},t)\\ &\quad=\sum_{\rm b}\hat{G}_{\rm ab}f_{\rm a}(\vec{r},\vec{k},t),\end{aligned} \tag{20}$$

where the distribution function $f_{\rm a}(\vec{r},\vec{k},t)$, multiplied with d^3rd^3k, defines the mean number of molecular species a within the volume element d^3r located at $\vec{r}$, whose wave vectors are confined within d^3k at $\vec{k}$, at time t. $n_{\rm a}(\vec{r},t)=\int d^3kf_{\rm a}(\vec{r},\vec{k},t)$ is the local number density and $N_{\rm a}=\int d^3rn_{\rm a}(\vec{r},t)$ stands for the total number of species a present in the system. In Eq. (20), $m_{\rm a}$ is the molecular mass of species a, $\vec{\nabla}_r=\hat{x}(\partial/\partial x)+\hat{y}(\partial/\partial y)+\hat{z}(\partial/\partial z)$, and $\vec{\nabla}_k=\hat{x}(\partial/\partial k_x)+\hat{y}(\partial/\partial k_y)+\hat{z}(\partial/\partial k_z)$. $\vec{F}^{\rm (a)}(\vec{r},t)$ stands for the external force acting on molecular species a. For ionic transport studies, in the absence of an external magnetic field, $\vec{F}^{\rm (a)}(\vec{r},t)$ is frequently equal to $Z_{\rm a}e\vec{E}^{\rm (ext)}(\vec{r},t)$, where e is the magnitude of the electric charge, $Z_{\rm a}$ is the charge number (positive or negative integers) of the species a, and $\vec{E}^{\rm (ext)}(\vec{r},t)$ is the external electric field. In Eq. (20), the symbol $\sum_{\rm b}\hat{G}_{\rm ab}$ stands for the nonlinear collision operator which, axiomatically, contains the complete information on molecular interactions taking place within the system. To proceed further, we here decompose the distribution function, $f_{\rm a}(\vec{r},\vec{k},t)$, as follows:

$$\begin{aligned}f_{\rm a}(\vec{r},\vec{k},t)&=f_{\rm a}^{\rm (eq)}(\vec{r},\vec{k},t)+f_{\rm a}^{\rm (neq)}(\vec{r},\vec{k},t)\\ &=n_{\rm a}^{\rm (eq)}(\vec{r},t)\phi_{\rm a}^{\rm (eq)}(k)+f_{\rm a}^{\rm (neq)}(\vec{r},\vec{k},t)\end{aligned} \tag{21}$$

$$\text{with}\quad\phi_{\rm a}^{\rm (eq)}(k)=\left(\frac{l_{\rm th}^{\rm (aa)}}{(2\pi)^{1/2}}\right)^3\exp\left[-\frac{1}{2}\left(l_{\rm th}^{\rm (aa)}k\right)^2\right], \tag{22}$$

where $f_a^{(neq)}(\vec{r},\vec{k},t)$ represents the space-time fluctuation in the distribution function from its values in the local thermal equilibrium, $l_{th}^{(ab)} = \hbar/\sqrt{2\mu_{ab}k_BT}$ and $\mu_{ab} = m_a m_b/(m_a + m_b)$. Notably, for equilibrium situations, we have assumed the local validity of the Maxwell-Boltzmann distribution of velocities and ignored the issue of quantum statistics, *if any*, for the moment.

A. Collision operator

A simple expression for $\hat{G}_{ab}$, using the *Stosszahlansatz* of Boltzmann and the framework of elastic quantum collisions among constituent species, is given as follows [85]:

$$\hat{G}_{ab} f_a(\vec{r},\vec{k},t) \approx -\xi_{ab} n_b^{(eq)}(\vec{r},t) f_a^{(neq)}(\vec{r},\vec{k},t), \tag{23}$$

$$\xi_{ab} = \left(\lambda_{th}^{(ab)}\right)^3 \omega_{th}[1 - {}_1F_1(2;1/2;-\xi_0)], \tag{24}$$

$$\xi_0 = 4\pi\left(s_{ab}/\lambda_{th}^{(ab)}\right)^2 = \left(p_{th}^{(ab)} s_{ab}/\hbar\right)^2 = \left(k_{th}^{(ab)} s_{ab}\right)^2, \tag{25}$$

where the symbol ${}_1F_1$ in Eq. (24) stands for the confluent hypergeometric function (Kummer function), $\omega_{th} = (2/\pi)k_BT/\hbar$, $\lambda_{th}^{(ab)} = [2\pi\hbar^2/(\mu_{ab}k_BT)]^{1/2}$, and s_{ab} is the range of the hard sphere potential, which may, in turn, be identified, particularly at low temperatures, with the scattering length, $l_{scat}^{(ab)}$, associated with the (a,b) pair of molecules. This identification is important for $l_{scat}^{(ab)}$, and s_{ab} can, in principle, differ by orders of magnitude [84], which may fruitfully be used to rationalize a variety of experimental observations, in particular, at low temperatures. $n_b^{(eq)}(\vec{r},t)$ is the time-dependent local equilibrium density of species b. $k_{th}^{(ab)}$ is the magnitude of thermal wave vector and $p_{th}^{(ab)}$ $(= \sqrt{2\mu_{ab}k_BT} = \hbar k_{th}^{(ab)}$, where μ_{ab} is the reduced mass) is the thermal momentum belonging to the pair of molecular species a and b. As an example, the value for $\lambda_{th}^{(ab)}$ for K^+ in water at 300 K is approximately equal to 0.03 nm, and therefore $k_{th}^{(ab)}$ is about 1.235×10^{11} m^{-1}. Notably, the argument, ξ_0, of the Kummer function in Eq. (24) possesses an interesting geometrical interpretation of quantum origin, for it refers to the area of the phase space which is spanned by the scattering length (a mechanical quantity) and the thermal momentum (a thermodynamic quantity) belonging to a pair of molecules, coarse grained over the Planck scale, as Eq. (25) reveals. Can this phase space area, represented by ξ_0, be exactly zero? This is possible when $s_{ab} = 0$ and this would happen when there are no interactions among molecular species in the system. In such a situation, the magnitude of the Kummer function is unity and hence $\xi_{ab} = 0$. For later use, we define a quantity, $g_{scat}^{(a)}$, of inverse length dimension, as given below:

$$g_{scat}^{(a)} \stackrel{def}{=} \left(\frac{m_a}{k_BT}\right)^{1/2} \sum_\beta \xi_{a\beta}\langle n_\beta^{(eq)}\rangle \Rightarrow \sum_\beta \xi_{a\beta}\langle n_\beta^{(eq)}\rangle = v_{th}^{(a)} g_{scat}^{(a)}, \tag{26}$$

where $v_{th}^{(a)} = (k_BT/m_a)^{1/2}$ and the summation index β stands for different species present in the system. In fact, $g_{scat}^{(a)}$ in Eq. (26) may be viewed as a fundamental attribute associated with the molecular species a, for which the explicit expression as given here in terms of $\xi_{a\beta}$ in Eq. (24), is an approximation, albeit a faithful one. In the absence of molecular interactions, however, $g_{scat}^{(a)} = 0$. In a complex molecular environment, as we will discuss later, $g_{scat}^{(a)}$ may depend on a number of physical variables. In a given circumstance, for analytical applications, the Kummer function, ${}_1F_1$, may be approximated as a finite series and accordingly Eq. (24) may be simplified, for limiting cases of the argument, ξ_0, as follows:

$$\xi_{ab} \approx 32\left(\frac{2\pi k_BT}{\mu_{ab}}\right)^{1/2} (s_{ab})^2 \tag{27}$$

$$\Rightarrow g_{scat}^{(a)} \approx 32\sqrt{2\pi}\sum_\beta \left(1 + \frac{m_a}{m_\beta}\right)^{1/2} (s_{a\beta})^2 \langle n_\beta^{(eq)}\rangle. \tag{28}$$

To estimate the order of magnitude for $g_{scat}^{(a)}$, let us consider K^+ in water at 0.01 M concentration. Given the number density of water, $\langle n_{H_2O}^{(eq)}\rangle = 3.3312 \times 10^{28}$ m^{-3} at 300 K, Eq. (28) yields $g_{scat}^{(K^+)} \approx 4.7576 \times 10^{30} \times (s_{K^+-H_2O})^2$ m^{-1}, where $s_{K^+-H_2O}$ is given in the unit of meter. A typical value for $s_{K^+-H_2O}$, as estimated from *ab initio* quantum chemical studies [87,88], is 0.165 nm (an approximate location of the repulsive wall), which implies $g_{scat}^{(K^+)} \approx 0.1295 \times 10^{12}$ m^{-1}.

Important remarks on the nature of s_{ab}, and therefore $g_{scat}^{(a)}$, and the possible scope for further generalizations are in order here. As it stands, the quantity s_{ab} refers to a pair of molecular species a and b, which are supposed to interact only with each other; that is, there are no external electromagnetic fields impressed on the molecular pair and also the pair does not interact with the internal fields generated by the surrounding electrically polarizable medium. In a complex molecular environment such as the embedding solvent, the crowded atmosphere of biological cells and so forth, however, s_{ab}, may, *inter alia*, depend on the local number density (equivalently, the concentration) of the molecular species. Then, obviously, if s_{ab} is a function of the number density, so must be the case with ξ_{ab} and consequently $g_{scat}^{(a)}$. In general, ξ_{ab} and $g_{scat}^{(a)}$ may be understood as a local quantity in the position space. How does s_{ab} depend on the local number density? This question is too complex to answer in full generality here. However, we note that the distance of closest approach, which the quantity s_{ab} essentially signifies, would obviously depend on the extent to which the embedding molecular atmosphere allows the pair (a, b) to approach each other. In the low-concentration regime (infinite dilution, say), for example, individual ions would be well surrounded by the solvent molecules and therefore the probability for two ions to be located in the close vicinity of each other would be smaller, in comparison to the circumstance when the electrolyte concentration is large and consequently there is a less effective solvation and caging of ions. In fact, the lowest limit on the distance of the closest approach (conceptually, the gas-phase limit wherein the pair (a, b) does not interact with the environment for all practical purposes) will be reached only when the electrolyte concentration is significantly large. Accordingly, we expect the magnitude of s_{ab} to decrease as the electrolyte concentration, $\langle n\rangle$, increases; that is, $ds_{ab}/d\langle n\rangle \leqslant 0$. For later use, we define an average quantity (positive-valued and dimensionless), θ_{av}, which is the

same for all pairs of molecules, as follows:

$$\frac{ds_{ab}}{d\langle n\rangle} + \theta_{av}\frac{s_{ab}}{\langle n\rangle} \approx 0. \tag{29}$$

At low electrolyte concentrations, s_{ab} is expected to be a slowly varying function of $\langle n\rangle$, and accordingly the magnitude of θ_{av} would be much less than unity. As an example, assuming a simple power-law dependence, an explicit model for the scattering length, $s_{ab}^{(min)} \leqslant s_{ab} \leqslant s_{ab}^{(max)}$, in the presence of complex molecular environments, may be given as follows:

$$s_{ab} = s_{ab}^{(max)} - \left(s_{ab}^{(max)} - s_{ab}^{(min)}\right)\left[\frac{\langle n\rangle - \langle n_{min}\rangle}{\langle n_{max}\rangle - \langle n_{min}\rangle}\right]^{\delta} \tag{30}$$

$$\Rightarrow \theta_{ab} = -\frac{\langle n\rangle}{s_{ab}}\frac{ds_{ab}}{d\langle n\rangle} = \delta\frac{\langle n_{max}\rangle - \langle n_{min}\rangle}{1 - \langle n_{min}\rangle/\langle n\rangle}\left(\frac{s_{ab}^{(max)}}{s_{ab}} - 1\right). \tag{31}$$

Then, θ_{av} in Eq. (29) may be taken as the average of θ_{ab}, as in Eq. (31), corresponding to all pairs of molecular species present in the system. In Eqs. (30) and (31), $\langle n_{min}\rangle$ stands for the electrolyte concentration at the infinite dilution, a physically realistic meaning of which will be discussed later, and $\langle n_{max}\rangle$ is the maximum electrolyte concentration that is physically conceivable for the electrolyte solution. Accordingly, $s_{ab}^{(min)}$ and $s_{ab}^{(max)}$ respectively stand for the minimum and maximum scattering length for the pair (a, b) in the given molecular environment. The exponent, δ, in Eq. (30), is a real and positive number ($\delta \geqslant 0$), which is to be determined by independent means (by appealing to experimental measurements, for example). For a slow variation of the scattering length with $\langle n\rangle$, the exponent may be taken in the range, $0 < \delta < 1$. Finally, anticipating the possibility of dynamical association and dissociation of electrolytes with the change of $\langle n\rangle$, s_{ab} may also be conceived as an oscillatory function (with decaying amplitude) of the local number density; that is, the equality in Eq. (29) would then potentially possess multiple roots and, for a given θ_{av}, there may be a number of concentration values of the electrolyte that would satisfy Eq. (29). Given Eq. (29), for later use, we obtain the slope of the $g_{scat}^{(a)}$ versus $\langle n_a^{(eq)}\rangle$ curve for the z:z-valent binary electrolyte (KCl, say) within the confinement of a solvent (H_2O, for example) as shown below. To be explicit, $g_{scat}^{(a)}$, from the simple expression in Eq. (28), reads as follows (with $\langle n_a^{(eq)}\rangle = \langle n\rangle = \langle n_b^{(eq)}\rangle$):

$$g_{scat}^{(a)} = 64\pi^{1/2}\left[\langle n\rangle\left\{(s_{aa})^2 + \frac{1}{\sqrt{2}}\left(1 + \frac{m_a}{m_b}\right)^{1/2}(s_{ab})^2\right\} + \frac{1}{\sqrt{2}}\langle n_s^{(eq)}\rangle\left(1 + \frac{m_a}{m_s}\right)^{1/2}(s_{as})^2\right] \tag{32}$$

$$\Rightarrow \frac{d}{d\langle n\rangle}g_{scat}^{(a)} \approx (1 - 2\theta_{av})\frac{g_{scat}^{(a)}}{\langle n\rangle}, \tag{33}$$

where $\langle n_s^{(eq)}\rangle$ is the equilibrium number density of the solvent, m_s is the mass of the solvent molecule, and s_{as} stands for the scattering length involving the charged molecular species a and the solvent molecule s. To reach Eq. (33), we have, for simplicity, assumed that the scattering length s_{as} is relatively independent of the solute concentration, $\langle n\rangle$.

Next, s_{ab}, at a given electrolyte concentration, may also depend on the (time-dependent) electromagnetic fields, which are either externally impressed or internally generated by the electromagnetically polarizable molecular medium. An important biophysical example, in the present context, is the voltage difference impressed along the ion channels in biological cells, that leads to a characteristic, and experimentally measurable, current-voltage response curve for the ion transport under study. Conceptually, then, s_{ab}, in general, should fluctuate in time. Though the exact mathematical expression for the dependence of s_{ab} on the voltage is not completely known here, we expect all physical scenarios to be probable and experimentally realizable; that is, the slope of the s_{ab} versus voltage curve may be either negative, zero, or positive. In such a situation, the mathematical analyses involving Eqs. (29)–(31) still hold if we simply substitute the variable, $\langle n\rangle$, by the voltage, with the understanding that θ_{av}, in Eq. (29), and the exponent, δ, in Eq. (30), would now admit all possible values (negative, zero, and positive). As we will see presently, it is, *inter alia*, the dependence s_{ab} on the local concentration and/or the electromagnetic fields, which reveals a rich variety of physical scenarios in specific examples of chemical and biophysical interests.

We now make a brief remark on the expression of the collision operator as given in Eqs. (23)–(25). This is a quantum mechanical result, based on plane waves as asymptotic scattering states, the use of which rests on the premise of the binary collision approximation of the Boltzmann transport equation. In a realistic physical situation, however, one may use distorted wave quantum scattering theory to obtain a better expression for the collision operator, though it is practically more complex to implement. The present treatment may be thought of as an approximation (plane wave) to the distorted wave description, the use of which is justified for the collisions that frequently dominate the physics is the short-range part of the interaction potential, wherein the molecular environments (such as the solvent) are essentially an average background effect. In the present work, we have attempted to ameliorate the situation by positing the scattering cross sections to be dependent on the concentration of the charged molecular species and the electromagnetic fields.

B. Nonequilibrium distribution function

To obtain an analytical expression for the distribution function, we substitute Eqs. (21) and (23) in Eq. (20), retain only those terms which are linear in the density of molecular species a, and express the Boltzmann equation in the Fourier

$(\vec{g},\omega)$ space as follows:

$$\left(-i\omega+\frac{i\hbar}{m_a}\vec{k}\cdot\vec{g}\right)f_a(\vec{g},\vec{k},\omega)+\frac{1}{(2\pi)^2}\iint d^3g'd^3\omega'\left\{\sum_b\frac{\xi_{ab}}{2}\left[n_b^{(eq)}(\vec{g}',\omega')f_a^{(neq)}(\vec{g}-\vec{g}',\vec{k},\omega-\omega')\right.\right.$$
$$\left.+n_b^{(eq)}(\vec{g}-\vec{g}',\omega-\omega')f_a^{(neq)}(\vec{g}',\vec{k},\omega')\right]\Bigg\}-\left\{\frac{\left(l_{th}^{(aa)}\right)^2}{2\hbar}\left[\vec{F}^{(a)}(\vec{g},\omega')\cdot\vec{k}n_a^{(eq)}(\vec{g}-\vec{g}',\omega-\omega')\right.\right.$$
$$\left.\left.+\vec{F}^{(a)}(\vec{g}-\vec{g}',\omega-\omega')\cdot\vec{k}n_a^{(eq)}(\vec{g}',\omega')\right]\phi_a^{(eq)}(k)\right\}=0. \tag{34}$$

Equation (34) is manifestly nonlinear, for the nonequilibrium fluctuation, $f_a^{(neq)}(\vec{g},\vec{k},\omega)$, which is as yet unknown, appears inside the integral. To obtain an analytically closed form expression for $f_a^{(neq)}(\vec{g},\vec{k},\omega)$, we evaluate the integrals in Eq. (34) with the following simplifying expression for the equilibrium density of molecular species b:

$$n_b^{(eq)}(\vec{g},\omega)\approx(2\pi)^2\langle n_b^{(eq)}\rangle\delta(\vec{g})\delta(\omega), \tag{35}$$

$$\text{with,}\quad\langle n_b^{(eq)}\rangle=\lim_{V\to\infty}\lim_{\tau\to\infty}\frac{1}{V\tau}\int_V\int_\tau d^3rdtn_b^{(eq)}(\vec{r},t), \tag{36}$$

where $(2\pi/\tau)\delta(\omega=0)\approx1\approx(8\pi^3/V)\delta(\vec{g}=0)$ with the understanding that V is the total volume available to the system and τ is the largest time scale relevant for the problem at hand. With Eq. (35), Eq. (34) yields the following expression for $f_a(\vec{g},\vec{k},\omega)$:

$$f_a(\vec{g},\vec{k},\omega)=\left[\left(i\sum_b\xi_{ab}\langle n_b^{(eq)}\rangle\right)n_a^{(eq)}(\vec{g},\omega)+i\frac{\left(l_{th}^{(aa)}\right)^2}{2\hbar}\frac{1}{(2\pi)^2}\iint d^3g'd^3\omega'\left\{\vec{k}\cdot\vec{F}^{(a)}(\vec{g}',\omega')n_a^{(eq)}(\vec{g}-\vec{g}',\omega-\omega')\right.\right.$$
$$\left.\left.+\vec{k}\cdot\vec{F}^{(a)}(\vec{g}-\vec{g}',\omega-\omega')n_a^{(eq)}(\vec{g}',\omega')\right\}\right]\frac{\phi_a^{(eq)}(k)}{\tilde{\omega}_a-\frac{\hbar}{m_a}\vec{k}\cdot\vec{g}}, \tag{37}$$

where $\tilde{\omega}_a=\omega+i\sum_b\xi_{ab}\langle n_b^{(eq)}\rangle=\omega+iv_{th}^{(a)}g_{scat}^{(a)}$. Equation (37) is an approximate solution of the Boltzmann equation in Eq. (20), which we use here to compute a number of observables.

V. OBSERVABLES

In what follows, we obtain analytically closed-form expression for the wave vector and frequency-dependent charge density, $\rho_a(\vec{g},\omega)$, transverse and longitudinal current density, $\vec{J}_\perp^{(a)}(\vec{g},\omega)/\vec{J}_{||}^{(a)}(\vec{g},\omega)$, and the coefficient of diffusion, $D_{||}^{(a)}(\vec{g},\omega)$, for molecular species a. In the sequel, we also obtain the space-time-averaged (that is, $\vec{g}=0$ and $\omega=0$) expressions for the same. As we will see presently, the longitudinal current density and the coefficient of diffusion, at zero frequency ($\omega=0$), are intimately related to each other.

A. Charge density

From Eq. (21), the number density, $n_a(\vec{g},\omega)$, of molecular species a in the Fourier $(\vec{g},\omega)$ space is given as follows:

$$n_a(\vec{g},\omega)=n_a^{(eq)}(\vec{g},\omega)+n_a^{(neq)}(\vec{g},\omega)=n_a^{(eq)}(\vec{g},\omega)+\int d^3kf_a^{(neq)}(\vec{g},\vec{k},\omega). \tag{38}$$

With Eq. (37) for $f_a^{(neq)}(\vec{g},\vec{k},\omega)$, Eq. (38) yields the following expression for the frequency and spatially dispersive number density:

$$n_a^{(neq)}(\vec{g},\omega)=\left[\left(1-\frac{\omega}{\tilde{\omega}_a}\right)\zeta_1^{(a)}(\vec{g},\omega)-1\right]n_a^{(eq)}(\vec{g},\omega)+\frac{i\lambda_a(\vec{g},\omega)}{2\hbar\tilde{\omega}_a}\left[\zeta_1^{(a)}(\vec{g},\omega)-1\right]\frac{1}{(2\pi)^2}$$
$$\times\iint d^3g'd^3\omega'\left[F_{||}^{(a)}(\vec{g}',\omega')n_a^{(eq)}(\vec{g}-\vec{g}',\omega-\omega')+F_{||}^{(a)}(\vec{g}-\vec{g}',\omega-\omega')n_a^{(eq)}(\vec{g}',\omega')\right], \tag{39}$$

where $F_{||}^{(a)}(\vec{g}',\omega')$ is the longitudinal (with respect to $\vec{g}$) component of the external force acting on species a and $\zeta_1^{(a)}(\vec{g},\omega)$ is as given below:

$$I_1^{(a)}(\vec{g},\omega)=\int_0^\infty dkk\phi_a^{(eq)}(k)\ln\left\{\frac{\tilde{\omega}_a+(\hbar kg/m_a)}{\tilde{\omega}_a-(\hbar kg/m_a)}\right\}, \tag{40}$$

$$\zeta_1^{(a)}(\vec{g},\omega)=2\pi\frac{I_1^{(a)}(\vec{g},\omega)}{l_{scat}^{(a)}(\vec{g},\omega)}=\sum_{s=0}^\infty\frac{\Gamma(2s)}{2^{s-1}\Gamma(s)}\left[l_{rel}^{(a)}(\vec{g},\omega)\right]^{2s}\approx2+\frac{k_BT}{H_{int}^{(a)}(\vec{g},\omega)}, \tag{41}$$

$$l_{\rm rel}^{(\rm a)}(\vec{g},\omega) = \frac{l_{\rm scat}^{(\rm a)}(\vec{g},\omega)}{l_{\rm th}^{(\rm aa)}} = \left(\frac{k_{\rm B}T}{H_{\rm int}^{(\rm a)}(\vec{g},\omega)}\right)^{1/2}, \tag{42}$$

$$l_{\rm scat}^{(\rm a)}(\vec{g},\omega) = \frac{g\hbar}{m_{\rm a}\tilde{\omega}_{\rm a}} \quad \text{and } H_{\rm int}^{(\rm a)}(\vec{g},\omega) = \frac{m_{\rm a}\tilde{\omega}_{\rm a}^2}{g^2}, \tag{43}$$

$$\text{and} \quad \lambda_{\rm a}(\vec{g},\omega) = \frac{l_{\rm th}^{(\rm aa)}}{l_{\rm rel}^{(\rm a)}(\vec{g},\omega)} = \frac{\hbar}{k_{\rm B}T}\frac{\tilde{\omega}_{\rm a}}{g}. \tag{44}$$

Next, if we evaluate the integral in Eq. (39) with the simplified expression for the equilibrium number density, $n_{\rm a}^{(\rm eq)}(\vec{g},\omega)$, as given in Eqs. (35) and (36), then $n_{\rm a}^{(\rm neq)}(\vec{g},\omega)$ in Eq. (39) takes the following form:

$$n_{\rm a}^{(\rm neq)}(\vec{g},\omega) = \left[\left(1-\frac{\omega}{\tilde{\omega}_{\rm a}}\right)\zeta_1^{(\rm a)}(\vec{g},\omega) - 1\right]n_{\rm a}^{(\rm eq)}(\vec{g},\omega) + \frac{i\lambda_{\rm a}(\vec{g},\omega)}{\hbar\tilde{\omega}_{\rm a}}\left(\zeta_1^{(\rm a)}(\vec{g},\omega)-1\right)F_{||}^{(\rm a)}(\vec{g},\omega)\langle n_{\rm a}^{(\rm eq)}\rangle \tag{45}$$

$$\Rightarrow \rho_{\rm a}^{(\rm neq)}(\vec{g},\omega) = Z_{\rm a}e n_{\rm a}^{(\rm neq)}(\vec{g},\omega) = \left[\left(1-\frac{\omega}{\tilde{\omega}_{\rm a}}\right)\zeta_1^{(\rm a)}(\vec{g},\omega) - 1\right]\rho_{\rm a}^{(\rm eq)}(\vec{g},\omega) + \frac{iZ_{\rm a}e}{\hbar\tilde{\omega}_{\rm a}}\lambda_{\rm a}(\vec{g},\omega)\left(\zeta_1^{(\rm a)}(\vec{g},\omega)-1\right)E_{||}^{(\rm ext)}(\vec{g},\omega)\langle\rho_{\rm a}^{(\rm eq)}\rangle \tag{46}$$

$$= \left[\left(1-\frac{\omega}{\tilde{\omega}_{\rm a}}\right)\zeta_1^{(\rm a)}(\vec{g},\omega) - 1\right]\rho_{\rm a}^{(\rm eq)}(\vec{g},\omega) + \epsilon_0[\kappa_{||}^{(\rm a)}(\vec{g},\omega)]^2\phi_{\rm ext}(\vec{g},\omega) \tag{47}$$

$$\text{where} \quad [\kappa_{||}^{(\rm a)}(\vec{g},\omega)]^2 = \frac{\lambda_{\rm a}(\vec{g},\omega)}{g}(g^2-\mu_0\epsilon_0\omega^2)\left[\zeta_1^{(\rm a)}(\vec{g},\omega)-1\right]\frac{Z_{\rm a}e\langle\rho_{\rm a}^{(\rm eq)}\rangle}{\epsilon_0\hbar\tilde{\omega}_{\rm a}} \tag{48}$$

$$\approx (Z_{\rm a}e)^2\frac{\langle n_{\rm a}^{(\rm eq)}\rangle}{\epsilon_0}\left[\frac{1}{H_{\rm int}^{(\rm a)}(\vec{g},\omega)}+\frac{1}{k_{\rm B}T}\right]\left[1-\mu_0\epsilon_0\left(\frac{\omega}{g}\right)^2\right] \tag{49}$$

$$\Rightarrow [\kappa_{||}^{(\rm a)}(\vec{g},\omega=0)]^2 \approx (Z_{\rm a}e)^2\frac{\langle n_{\rm a}^{(\rm eq)}\rangle}{\epsilon_0 k_{\rm B}T}\left[1-\left(\frac{g}{g_{\rm scat}^{(\rm a)}}\right)^2\right] \tag{50}$$

$$= \left[1-\left(\frac{g}{g_{\rm scat}^{(\rm a)}}\right)^2\right]\times(Z_{\rm a}\times 2.0531\,{\rm nm}^{-1})^2 \ \ (0.01\ {\rm M\ solution\ at\ 300\,K}). \tag{51}$$

To pass from Eq. (46) to Eq. (47), we have used the expression for the longitudinal electric field, $E_{||}^{(\rm ext)}(\vec{g},\omega)$, as given in Eq. (17). The symbols ϵ_0 and μ_0 in Eqs. (47) and (48) respectively stands for the permittivity and the permeability of the surrounding medium (vacuum, here). The quantity, $1/\kappa_{||}^{(\rm a)}(\vec{g},\omega)$, from Eq. (48), defines a characteristic *longitudinal length* scale of the system, which transcends the notion of *Debye length*, frequently used in electrochemical sciences. Using Eqs. (38) and (46)–(48), now, the total charge density, $\rho_{\rm tot}(\vec{g},\omega)$, may be obtained by summing $\rho_{\rm s}(\vec{g},\omega)[=\rho_{\rm s}^{(\rm eq)}(\vec{g},\omega)+\rho_{\rm s}^{(\rm neq)}(\vec{g},\omega)]$ over all molecular species s present in the system, as shown below:

$$\rho_{\rm tot}(\vec{g},\omega) = \rho_{\rm tot}^{(\rm Diff)}(\vec{g},\omega) + \rho_{\rm tot}^{(\rm Drift)}(\vec{g},\omega), \tag{52}$$

$$\rho_{\rm tot}^{(\rm Diff)}(\vec{g},\omega) = \sum_{\rm s}\left(1-\frac{\omega}{\tilde{\omega}_{\rm s}}\right)\zeta_1^{(\rm s)}(\vec{g},\omega)\rho_{\rm s}^{(\rm eq)}(\vec{g},\omega), \tag{53}$$

$$\rho_{\rm tot}^{(\rm Drift)}(\vec{g},\omega) = \epsilon_0[\kappa_{||}(\vec{g},\omega)]^2\phi_{\rm ext}(\vec{g},\omega), \tag{54}$$

$$[\kappa_{||}(\vec{g},\omega)]^2 = \sum_{\rm s}[\kappa_{||}^{(\rm s)}(\vec{g},\omega)]^2. \tag{55}$$

In the long-wavelength limit, we have $(g/g_{\rm scat}^{(\rm a)})^2 \ll 1$ [for example, at 300 K, $g_{\rm scat}^{(\rm K^+)} \approx 0.1295\times10^{12}\,{\rm m}^{-1}$ from Eq. (28)] and therefore the value of $1/\kappa_{||}^{(\rm a)}$ in Eq. (51) is approximately equal to 0.49 nm for potassium ions in aqueous solvent. In fact, Eq. (49) yields, for $g = 1\,{\rm nm}^{-1}$ and 0.01 M solution, $\kappa_{||}^{(\rm K^+)}(\vec{g},\omega = k_{\rm B}T/\hbar) \approx 2.05\times(1-i0.24\times10^{-4})\,{\rm nm}^{-1}$.

To unfold the essential characteristics of the $[\kappa_{||}^{(\rm a)}(\vec{g},\omega)]^2$ versus $\langle n_{\rm a}^{(\rm eq)}\rangle$ curve, let us, for simplicity, consider Eq. (48) with $\omega = 0$ for the case of z:z-valent electrolyte solution, assuming $g < g_{\rm scat}^{(\rm a)}$. To this end, we use Eqs. (33) and (48) to compute the slope as follows:

$$\frac{d}{d\langle n_{\rm a}^{(\rm eq)}\rangle}[\kappa_{||}^{(\rm a)}(\vec{g},\omega=0)]^2 \approx \frac{(Z_{\rm a}e)^2}{\epsilon k_{\rm B}T}\left(\frac{2g}{g_{\rm scat}^{(\rm a)}}\right)^2(\theta_c-\theta_{\rm av}), \tag{56}$$

where $4\theta_c = 1+(g_{\rm scat}^{(\rm a)}/g)^2$. From Eq. (56), we may now draw a number of conclusions. As we have discussed earlier [see the arguments following Eq. (29)], $\theta_{\rm av}$, at very low concentrations, is expected to be an infinitesimally small (positive) number. Accordingly, then, from Eq. (56), the slope of the $[\kappa_{||}^{(\rm a)}(\vec{g},\omega=0)]^2$ versus $\langle n_{\rm a}^{(\rm eq)}\rangle$ curve will be positive, as we expect for electrolyte solutions in the low-concentration region, which is also consistent with the predictions of

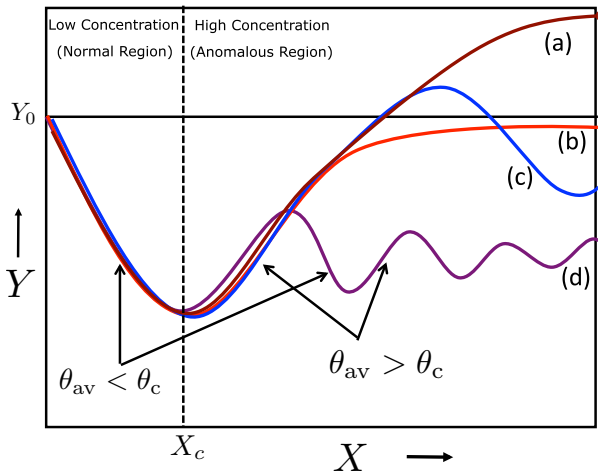

FIG. 1. A schematic plot for various equations of state. $Y/X = [1/\kappa_{||}^{(a)}(\vec{g},\omega)]/\langle n_a^{(eq)}\rangle$ (only curve d, Y_0 = a large positive number), $\ln\gamma/\langle n\rangle$ (all curves, $Y_0 = 0$), $\Lambda_m/\langle n\rangle$ (only curve d, Y_0 = molar conductivity at infinite dilution), and $D_{||}^{(a)}/\langle n_a^{(eq)}\rangle$ (only curve d, Y_0 = a finite positive number) for the situation when the extremum condition, $\theta_{av} = \theta_c$ (for each Y/X pair) is satisfied for a number of concentration values (X_c is the corresponding critical concentration). The normal region, which falls within the predictions of the Debye-Hückel-Onsager phenomenology, lies between the zero concentration and the first extremum, whereas the region beyond the first extremum is the high-concentration regime, displaying a variety of anomalies.

the DHO paradigm. If, on the other hand, $\theta_{av} > \theta_c$, which will be the case at high concentrations, the slope will be negative, which implies that the characteristic length scale, $1/\kappa_{||}^{(a)}(\vec{g},\omega = 0)$, which is analogous to the Debye length, will increase as the electrolyte concentration increases. This is the *anomalous regime*, which is not covered by the DHO phenomenology and its variants. Next, the situation $\theta_{av} = \theta_c$ may, in general, yield a number of nontrivial roots (extrema); that is, the equality would, in general, be satisfied for a number of physically realizable concentration values of the electrolyte. In general, then, we expect an oscillatory behavior for the $1/\kappa_{||}^{(a)}(\vec{g},\omega)$ versus $\langle n_a^{(eq)}\rangle$ curve, as schematically shown Fig. 1 (curve d).

As indicated in Fig. 1, the region between the lowest concentration and the first extremum, which is a minimum here, is what falls under the DHO phenomenology. Beyond the first extremum lies the anomalous regime, the existence of which is interestingly seen in a recent experimental work on NaCl in water and an ionic liquid (1-butyl-1-methylpyrrolidinium bis[(trifluoromethane)-sulfonyl]imide, $[C_4C_1Pyrr][NTf_2]$) solution in propylene carbonate at high concentrations [82]. In this experiment, the first extremum for the NaCl and ionic liquid solutions are found at about 1 and 0.64 M respectively. Even more interesting in the experimental findings on ionic liquid solution is the appearance of a second extremum (at about 2.75 M) [82], which essentially indicates an oscillatory behavior for the $1/\kappa_{||}^{(a)}(\vec{g},\omega)$ versus $\langle n_a^{(eq)}\rangle$ curve, consistent with the present analysis. This oscillatory behavior may be attributed to the process of caging and decaging ions by the solvent molecules as the electrolyte concentration increases. Finally, for $\vec{g} = 0$, the nonequilibrium density is obtained as follows: $\tilde{\omega}_a\rho_a^{(neq)}(\vec{g} = 0,\omega) + \omega\rho_a^{(eq)}(\vec{g} = 0,\omega) = 0$, which implies $\rho_a^{(neq)}(\vec{g} = 0,\omega = 0) = 0 \Rightarrow \langle\rho_a^{(neq)}\rangle = 0$. The total density, $\rho_{tot}(\vec{g} = 0,\omega) = \sum_s(1 - \omega/\tilde{\omega}_s)\rho_s^{(eq)}(\vec{g} = 0,\omega) \Rightarrow \rho_{tot}(\vec{g} = 0,\omega = 0) = \sum_s \rho_s^{(eq)}(\vec{g}=0,\omega = 0) = (2\pi)^4\delta(\vec{g}=0)\,\delta(\omega = 0)\sum_s\langle\rho_s^{(eq)}\rangle = 0$, if the system is electrically neutral.

B. Transverse current density

The expression for the transverse current density, in the Fourier $(\vec{g},\omega)$ space, is, by definition, given as the nonequilibrium average of the transverse current as follows:

$$\vec{J}_\perp^{(a)}(\vec{g},\omega) = Z_a e\int_{-\infty}^{\infty} d^3k\frac{\hbar\vec{k}_\perp}{m_a}f_a(\vec{g},\vec{k},\omega) = Z_a e\frac{\hbar}{m_a}\int_{-\infty}^{\infty} d^3k\vec{k}_\perp f_a^{(neq)}(\vec{g},\vec{k},\omega) \tag{57}$$

To comply with the constitution relation, $\vec{J}_\perp^{(a)}(\vec{g},\omega) = \sigma_\perp^{(a)}(\vec{g},\omega)\vec{E}_\perp^{(ext)}(\vec{g},\omega)$ in Eq. (4), we substitute $f_a^{(neq)}(\vec{g},\vec{k},\omega)$ from Eq. (37) in Eq. (57), use $\vec{F}^{(a)}(\vec{g},\omega) = Z_a e\vec{E}^{(ext)}(\vec{g},\omega)$, and perform the integral for $\vec{k}$ fully analytically. The final expression for the transverse current density is as follows:

$$\vec{J}_\perp^{(a)}(\vec{g},\omega) = (Z_a e)^2\frac{\left(l_{th}^{(aa)}\right)^2}{2\hbar}\frac{i}{2g}\left[\frac{m_a\tilde{\omega}_a}{g\hbar} + 2\pi\left\{I_2^{(a)}(\vec{g},\omega) - \left(\frac{m_a\tilde{\omega}_a}{g\hbar}\right)^2 I_1^{(a)}(\vec{g},\omega)\right\}\right]$$
$$\times\frac{1}{(2\pi)^2}\iint d^3g'd\omega'\left\{n_a^{(eq)}(\vec{g}-\vec{g}',\omega-\omega')\vec{E}_\perp^{(ext)}(\vec{g}',\omega') + n_a^{(eq)}(\vec{g}',\omega')\vec{E}_\perp^{(ext)}(\vec{g}-\vec{g}',\omega-\omega')\right\}, \tag{58}$$

where $\vec{E}_\perp^{(ext)}(\vec{g}',\omega)$ is the transverse (with respect to $\vec{g}$) external electric field. The expression for $I_1^{(a)}(\vec{g},\omega)$ is as shown in Eq. (40), whereas $I_2^{(a)}(\vec{g},\omega)$ is as given below:

$$I_2^{(a)}(\vec{g},\omega) = \int_0^\infty dkk^3\phi_a^{(eq)}(k)\ln\left\{\frac{\tilde{\omega}_a + (\hbar kg/m_a)}{\tilde{\omega}_a - (\hbar kg/m_a)}\right\} = \frac{1}{2\pi}\frac{\zeta_2^{(a)}(\vec{g},\omega)}{l_{scat}^{(a)}(\vec{g},\omega)} \tag{59}$$

$$\text{with}\quad \zeta_2^{(\mathrm{a})}(\vec{g},\omega)=\sum_{s=0}^{\infty}\frac{(2s+3)\Gamma(2s)}{2^{s-1}\Gamma(s)}\left[l_{\mathrm{rel}}^{(\mathrm{a})}(\vec{g},\omega)\right]^{2s+2}\approx\frac{6k_{\mathrm{B}}T}{H_{\mathrm{int}}^{(\mathrm{a})}(\vec{g},\omega)}, \tag{60}$$

where $H_{\mathrm{int}}^{(\mathrm{a})}(\vec{g},\omega)$ is as given in Eq. (43). With Eqs. (59) and (60), Eq. (58) for the transverse current density reduces to the following form:

$$\vec{J}_{\perp}^{(\mathrm{a})}(\vec{g},\omega)=\frac{i\lambda_{\mathrm{a}}(\vec{g},\omega)}{4g\hbar}(Z_ae)^2\left[1+\zeta_2^{(\mathrm{a})}(\vec{g},\omega)-\zeta_1^{(\mathrm{a})}(\vec{g},\omega)\right]\frac{1}{(2\pi)^2}\iint d^3g'd\omega'\left\{n_{\mathrm{a}}^{(\mathrm{eq})}(\vec{g}-\vec{g}',\omega-\omega')\vec{E}_{\perp}^{(\mathrm{ext})}(\vec{g}',\omega')\right.$$
$$\left.+n_{\mathrm{a}}^{(\mathrm{eq})}(\vec{g}',\omega')\vec{E}_{\perp}^{(\mathrm{ext})}(\vec{g}-\vec{g}',\omega-\omega')\right\} \tag{61}$$

$$\Rightarrow\sigma_{\perp}^{(\mathrm{a})}(\vec{g},\omega)=\frac{i\lambda_{\mathrm{a}}(\vec{g},\omega)}{4g\hbar}(Z_ae)^2\left[1+\zeta_2^{(\mathrm{a})}(\vec{g},\omega)-\zeta_1^{(\mathrm{a})}(\vec{g},\omega)\right]\frac{1}{E_{\perp}^{(\mathrm{ext})}(\vec{g},\omega)}\frac{1}{(2\pi)^2}\iint d^3g'd\omega'\left[n_{\mathrm{a}}^{(\mathrm{eq})}(\vec{g}-\vec{g}',\omega-\omega')\vec{E}_{\perp}^{(\mathrm{ext})}(\vec{g}',\omega')\right.$$
$$\left.+n_{\mathrm{a}}^{(\mathrm{eq})}(\vec{g}',\omega')\vec{E}_{\perp}^{(\mathrm{ext})}(\vec{g}-\vec{g}',\omega-\omega')\right]\cdot\hat{E}_{\perp}^{(\mathrm{ext})}(\vec{g},\omega), \tag{62}$$

where $\lambda_{\mathrm{a}}(\vec{g},\omega)$ is as given in Eq. (44) and $\hat{E}_{\perp}^{(\mathrm{ext})}(\vec{g},\omega)$ is the unit vector in the transverse direction. Now, Eqs. (61) and (62) involve a convolution of the external electric field with the equilibrium number density for species a, which may be further simplified if we use the approximation for $n_a^{(\mathrm{eq})}(\vec{g},\omega)$ as expressed in Eqs. (35) and (36). Accordingly, then, the expression for the transverse current in Eq. (61) and the transverse conductivity in Eq. (62) reduce to the following mathematical form:

$$\vec{J}_{\perp}^{(\mathrm{a})}(\vec{g},\omega)=\sigma_{\perp}^{(\mathrm{a})}(\vec{g},\omega)\vec{E}_{\perp}^{(\mathrm{ext})}(\vec{g},\omega) \tag{63}$$

$$\text{where}\quad \sigma_{\perp}^{(\mathrm{a})}(\vec{g},\omega)=\frac{iZ_ae\lambda_{\mathrm{a}}(\vec{g},\omega)}{2g\hbar}\left[1+\zeta_2^{(\mathrm{a})}(\vec{g},\omega)-\zeta_1^{(\mathrm{a})}(\vec{g},\omega)\right]\left\langle\rho_{\mathrm{a}}^{(\mathrm{eq})}\right\rangle. \tag{64}$$

Furthermore, if we use the approximations as indicated in Eqs. (41) and (60), Eq. (64) simplifies as follows:

$$\sigma_{\perp}^{(\mathrm{a})}(\vec{g},\omega)\approx\frac{i}{2}(Z_ae)^2\frac{\left\langle n_{\mathrm{a}}^{(\mathrm{eq})}\right\rangle}{m_{\mathrm{a}}\tilde{\omega}_{\mathrm{a}}}\left(5-\frac{H_{\mathrm{int}}^{(\mathrm{a})}(\vec{g},\omega)}{k_{\mathrm{B}}T}\right) \tag{65}$$

$$\Rightarrow\sigma_{\perp}^{(\mathrm{a})}(\vec{g},\omega=0)\approx\frac{(Z_ae)^2}{2(m_ak_{\mathrm{B}}T)^{1/2}}\frac{\left\langle n_{\mathrm{a}}^{(\mathrm{eq})}\right\rangle}{g_{\mathrm{scat}}^{(\mathrm{a})}}\left[5+\left(\frac{g_{\mathrm{scat}}^{(\mathrm{a})}}{g}\right)^2\right], \tag{66}$$

where $g_{\mathrm{scat}}^{(\mathrm{a})}$ is as given in Eq. (26) or Eq. (28). In the long-wavelength limit with $g=10^9\,\mathrm{m}^{-1}$ and 0.01 M solution at 300 K temperature, for example, Eq. (65) yields $\sigma_{\perp}^{(\mathrm{K}^+)}(\vec{g},\omega=k_{\mathrm{B}}T/\hbar)\approx 611\times(1-i1.2)$ S m^{-1}, whereas Eq. (65) gives $\sigma_{\perp}^{(\mathrm{K}^+)}(\vec{g},\omega=0)\approx 611$ S m^{-1}. Next, we use Eq. (18) to express $\vec{E}_{\perp}^{(\mathrm{ext})}(\vec{g},\omega)$ in Eq. (63) in terms of the transverse vector potential, $\vec{A}_{\perp}^{(\mathrm{ext})}(\vec{g},\omega)$, and introduce the notion of a characteristic *transverse length* (analogous to the *Debye length*), $\kappa_{\perp}^{(\mathrm{a})}(\vec{g},\omega)$, associated with the molecular species a, as follows:

$$\vec{J}_{\perp}^{(\mathrm{a})}(\vec{g},\omega)=\mu^{-1}[\kappa_{\perp}^{(\mathrm{a})}(\vec{g},\omega)]^2\vec{A}_{\perp}^{(\mathrm{ext})}(\vec{g},\omega),$$
$$\text{with}\quad [\kappa_{\perp}^{(\mathrm{a})}(\vec{g},\omega)]^2=i\mu\omega\sigma_{\perp}^{(\mathrm{a})}(\vec{g},\omega). \tag{67}$$

With $g=1\,\mathrm{nm}^{-1}$ and 0.01 M solution at 300 K, Eqs. (65)–(67) yield the transverse length scale, $1/\kappa_{\perp}^{(\mathrm{K}^+)}(\vec{g},\omega=k_{\mathrm{B}}T/\hbar)\approx 4.33\times(1-i0.36)\times10^{-6}$ m, as opposed to the value $0.49\times(1+i0.24\times10^{-4})\times10^{-9}$ m for the longitudinal length scale (see Sec. V A). That means, in the long-wavelength limit, the molecular ions are essentially well shielded along the longitudinal direction, as opposed to the transverse one.

Next, we note that Eqs. (58)–(67) are valid only for nonzero wave vector (that is, $\vec{g}\neq 0$). For $\vec{g}=0$, on the other hand, the expressions for the transverse current density and the conductivity are obtained as follows:

$$\vec{J}_{\perp}^{(\mathrm{a})}(\vec{g}=0,\omega)=Z_ae\int_{-\infty}^{\infty}d^3k\frac{\hbar\vec{k}_{\perp}}{m_{\mathrm{a}}}f_{\mathrm{a}}^{(\mathrm{neq})}(\vec{g}=0,\vec{k},\omega) \tag{68}$$

$$=\frac{iZ_ae}{2\pi m_{\mathrm{a}}\tilde{\omega}_{\mathrm{a}}}\frac{1}{(2\pi)^2}\iint d^3g'd\omega'\times\left\{\rho_{\mathrm{a}}^{(\mathrm{eq})}(-\vec{g}',\omega-\omega')\vec{E}_{\perp}^{(\mathrm{ext})}(\vec{g}',\omega')+\rho_{\mathrm{a}}^{(\mathrm{eq})}(\vec{g}',\omega')\vec{E}_{\perp}^{(\mathrm{ext})}(-\vec{g}',\omega-\omega')\right\} \tag{69}$$

$$\approx\frac{iZ_ae\left\langle\rho_{\mathrm{a}}^{(\mathrm{eq})}\right\rangle}{\pi m_{\mathrm{a}}\tilde{\omega}_{\mathrm{a}}}\vec{E}_{\perp}^{(\mathrm{ext})}(\vec{g}=0,\omega) \tag{70}$$

$$\Rightarrow\vec{J}_{\perp}^{(\mathrm{a})}(\vec{g}=0,\omega=0)\approx\frac{Z_ae\left\langle\rho_{\mathrm{a}}^{(\mathrm{eq})}\right\rangle}{\pi m_{\mathrm{a}}\sum_{\mathrm{b}}\xi_{\mathrm{ab}}\left\langle n_{\mathrm{b}}^{(\mathrm{eq})}\right\rangle}\times\vec{E}_{\perp}^{(\mathrm{ext})}(\vec{g}=0,\omega=0) \tag{71}$$

$$\Rightarrow\left\langle\vec{J}_{\perp}^{(\mathrm{a})}\right\rangle=\sigma_{\mathrm{a}}\left\langle\vec{E}_{\perp}^{(\mathrm{ext})}\right\rangle,$$
$$\text{where}\quad \sigma_{\mathrm{a}}\approx\frac{1}{\pi}\frac{(Z_ae)^2}{(m_ak_{\mathrm{B}}T)^{1/2}}\frac{\left\langle n_{\mathrm{a}}^{(\mathrm{eq})}\right\rangle}{g_{\mathrm{scat}}^{(\mathrm{a})}}. \tag{72}$$

To pass from Eq. (68) to Eq. (69), we have used Eq. (37) with $\vec{g}=0$ for $f_{\mathrm{a}}^{(\mathrm{neq})}(\vec{g}=0,\vec{k},\omega)$ and performed the integral over $\vec{k}$ fully analytically. Next, to go from Eq. (69) to Eq. (70), we have used the simplifying expression for the equilibrium number density as given in Eqs. (35) and (36). Finally, we have used the relation given in Eq. (26) to pass from Eq. (71) to Eq. (72). Equation (72) is the simplest expression for the

average conductivity that contains the complete information on scattering events, through $g^{(a)}_{scat}$ as given in Eq. (26) or Eq. (28), involving charged molecular species constituting the system. For 0.01 M aqueous solution of KCl at 300 K, Eq. (72) yields $\sigma_{K^+} \approx 0.023$ S m^{-1}, the experimental context of which will be will be given later (see Sec. VIII C).

An important remark regarding the temperature dependence of the conductivity, σ_a, in Eq. (72), is in order here. First, for a given electrolyte solution, we note that the summation over β in Eq. (26), which defines $g^{(a)}_{scat}$, involves the solvent molecules, beside the ions constituting the electrolyte. That means $g^{(a)}_{scat}$, as Eqs. (24) and (26) reveal, has an explicit dependence on temperature through the argument of the Kummer function, beside an implicit dependence through the solvent density. Furthermore, as Eq. (28) reveals, $g^{(a)}_{scat}$, in the lowest order of approximation, has only implicit dependence on temperature through the solvent density. Now, the solvent density, in most circumstances (except, for example, the temperature range where water displays anomalies), is expected to decrease with the increase of temperature, which, from Eq. (28), means that $g^{(a)}_{scat}$ would also decrease with the temperature. It may happen that $g^{(a)}_{scat}$ has a power-law dependence; that is, $g^{(a)}_{scat} \propto T^{\delta-1/2}$ (with $\delta \leqslant 1/2$). It may also happen that the explicit and implicit dependences compensate each other in such as way that $\delta = 1/2$ and consequently $g^{(a)}_{scat}$ becomes temperature independent. Keeping in view these possible scenarios, Eq. (72) reveals a rich set of possibilities. If δ is a negative number, then the conductivity, σ_a, will increase with the increase of temperature, as we normally expect. Next, the situation $\delta = 0$ implies a plateau region for the σ_a versus T curve. If, however, δ happens to assume a positive value then the σ_a versus T curve would anomalously exhibit a negative slope, which may be verified in experiments.

C. Longitudinal current density and diffusion

The longitudinal current density is defined as the nonequilibrium average of the longitudinal current, which, in the Fourier $(\vec{g},\omega)$ space, is given as follows:

$$\vec{J}^{(a)}_{\parallel}(\vec{g},\omega) = Z_a e \int d^3k \frac{\hbar \vec{k}_{\parallel}}{m_a} f_a(\vec{g},\vec{k},\omega) = \frac{Z_a e\hbar}{m_a} \int d^3k \vec{k}_{||} f^{(neq)}_a(\vec{g},\vec{k},\omega). \quad (73)$$

In accordance with the constitutive relation in Eq. (3), we substitute $f^{(neq)}_a(\vec{g},\vec{k},\omega)$ from (37) in Eq. (73) with $\vec{F}^{(a)}(\vec{g},\omega) = Z_a e \vec{E}^{(ext)}_{||}(\vec{g},\omega)$ and perform the integral over $\vec{k}$ fully analytically to obtain the following expression for the longitudinal current density:

$$\vec{J}^{(a)}_{\parallel}(\vec{g},\omega) = Z_a e\big(\zeta^{(a)}_1(\vec{g},\omega)-1\big)\Big[(\tilde{\omega}_a-\omega)\frac{\hat{g}}{g} n^{(eq)}_a(\vec{g},\omega) + \frac{i Z_a e \lambda_a(\vec{g},\omega)}{2g\hbar}\frac{1}{(2\pi)^2}\iint d^3g' d\omega' \times \big\{n^{(eq)}_a(\vec{g}-\vec{g}',\omega-\omega')\vec{E}^{(ext)}_{||}(\vec{g}',\omega') + n^{(eq)}_a(\vec{g}',\omega')\vec{E}^{(ext)}_{||}(\vec{g}-\vec{g}',\omega-\omega')\big\}\Big] \quad (74)$$

where, $\vec{E}^{(ext)}_{||}(\vec{g}',\omega') = [\hat{g}\cdot\vec{E}^{(ext)}(\vec{g}',\omega')]\hat{g}$. (75)

The first term on the right-hand side of Eq. (74) is the diffusion current density arising because of the density (equivalently, the concentration) gradient present in the system, whereas the second term stands for the pure conduction current density due to the externally applied longitudinal electric field, $\vec{E}^{(ext)}_{||}(\vec{g},\omega)$. To extract the expressions for the coefficient of diffusion, $D^{(a)}_{||}(\vec{g},\omega)$, and the longitudinal conductivity, $\sigma^{(a)}_{||}(\vec{g},\omega)$, we use the constitutive relations, Eqs. (3) and (5), in Eq. (74). The final results are as given below:

$$D^{(a)}_{||}(\vec{g},\omega) = \frac{i(\tilde{\omega}_a-\omega)}{g^2}\big(\zeta^{(a)}_1(\vec{g},\omega)-1\big)\frac{n^{(eq)}_a(\vec{g},\omega)}{n_a(\vec{g},\omega)}, \quad (76)$$

$$\sigma^{(a)}_{||}(\vec{g},\omega) = \frac{i\lambda_a(\vec{g},\omega)}{2g\hbar}(Z_a e)^2\frac{\zeta^{(a)}_1(\vec{g},\omega)-1}{E^{(ext)}_{||}(\vec{g},\omega)}\frac{1}{(2\pi)^2} \times \iint d^3g' d\omega'\big[n^{(eq)}_a(\vec{g}-\vec{g}',\omega-\omega')\vec{E}^{(ext)}_{||}(\vec{g}',\omega') + n^{(eq)}_a(\vec{g}',\omega')\vec{E}^{(ext)}_{||}(\vec{g}-\vec{g}',\omega-\omega')\big]\cdot\hat{E}^{||}_{ext}(\vec{g},\omega). \quad (77)$$

Equation (77) may be further simplified if we use Eqs. (35) and (36) for $n^{(eq)}_a(\vec{g},\omega)$, in which case the final results are as given below:

$$\sigma^{(a)}_{||}(\vec{g},\omega) = \frac{i\lambda_a(\vec{g},\omega)}{g\hbar}(Z_a e)^2\big(\zeta^{(a)}_1(\vec{g},\omega)-1\big)\big\langle n^{(eq)}_a\big\rangle, \quad (78)$$

where $\vec{J}^{(a)}_{\parallel}(\vec{g},\omega) = \sigma^{(a)}_{||}(\vec{g},\omega)\vec{E}^{(ext)}_{||}(\vec{g},\omega) - igD^{(a)}_{||}(\vec{g},\omega)\rho_a(\vec{g},\omega)\hat{g}$ (79)

$$= \{(\epsilon_0\tilde{\omega}_a)[\kappa^{(a)}_{||}(\vec{g},\omega)]^2\phi_{ext}(\vec{g},\omega) - ig^2 D^{(a)}_{||}(\vec{g},\omega)\rho_a(\vec{g},\omega)\}\frac{\hat{g}}{g} \quad (80)$$

with $[\kappa^{(a)}_{||}(\vec{g},\omega)]^2 = i\left(\frac{\mu_0\epsilon_0\omega^2-g^2}{\tilde{\omega}_a\epsilon_0}\right)\sigma^{(a)}_{||}(\vec{g},\omega)$. (81)

Notably, $\kappa^{(a)}_{||}(\vec{g},\omega)$ in Eqs. (80) and (81) stands for the characteristic *longitudinal length* (analogous to the *Debye length*), which is the same as that given in Eq. (48). Next, if we use the approximation as indicated in Eq. (41), the coefficient of diffusion in Eq. (76) and the longitudinal conductivity in Eq. (78) assume the following forms:

$$D^{(a)}_{||}(\vec{g},\omega) \approx \frac{i(\tilde{\omega}_a-\omega)}{g^2}\left(1+\frac{g^2k_BT}{m_a\tilde{\omega}^2_a}\right)\frac{n^{(eq)}_a(\vec{g},\omega)}{n_a(\vec{g},\omega)} \quad (82)$$

$$\Rightarrow D^{(a)}_{||}(\vec{g},\omega=0) \approx \frac{v^{(a)}_{th}}{g^{(a)}_{scat}}\left[1-\left(\frac{g^{(a)}_{scat}}{g}\right)^2\right]\frac{n^{(eq)}_a(\vec{g},\omega=0)}{n_a(\vec{g},\omega=0)} \quad (83)$$

$$\approx \frac{v_{\rm th}^{(\rm a)}}{g_{\rm scat}^{(\rm a)}}\left[1-\left(\frac{g_{\rm scat}^{(\rm a)}}{g}\right)^2\right], \tag{84}$$

$$\sigma_{||}^{(\rm a)}(\vec{g},\omega) \approx i(Z_{\rm a}e)^2\frac{\langle n_{\rm a}^{(\rm eq)}\rangle}{m_{\rm a}\tilde{\omega}_{\rm a}}\left(1+\frac{H_{\rm int}^{(\rm a)}(\vec{g},\omega)}{k_{\rm B}T}\right), \tag{85}$$

$$\sigma_{||}^{(\rm a)}(\vec{g},\omega=0) \approx \frac{(Z_{\rm a}e)^2}{m_{\rm a}}\frac{\langle n_{\rm a}^{(\rm eq)}\rangle}{v_{\rm th}^{(\rm a)}\,g_{\rm scat}^{(\rm a)}}\left[1-\left(\frac{g_{\rm scat}^{(\rm a)}}{g}\right)^2\right]. \tag{86}$$

To go from Eq. (83) to Eq. (84), we have used the approximation implied by Eqs. (35) and (36) and the fact that $\langle\rho_{\rm a}^{(\rm neq)}\rangle = 0$ and therefore $\langle n_{\rm a}\rangle = \langle n_{\rm a}^{(\rm eq)}\rangle$. Now, upon comparing Eqs. (84) and (86), we have the following interesting relation, analogous to the Nernst-Einstein equation, well known in electrochemical science [2], between the longitudinal conductivity and the diffusion coefficient: $D_{||}^{(\rm a)}(\vec{g},\omega=0) = \frac{1}{(z_{\rm a}e)^2\langle n_{\rm a}\rangle}\frac{\partial}{\partial[1/(k_{\rm B}T)]}[\sigma_{||}^{(\rm a)}(\vec{g},\omega=0)]$. That is, the slope of the $\sigma_{||}^{(\rm a)}(\vec{g},\omega=0)$ versus $1/(k_{\rm B}T)$ curve may be used to extract the coefficient of diffusion from the experimentally obtained longitudinal conductivity as a function of temperature. Next, for a substantial diffusive transport processes, one must have a significantly large concentration gradient present in the system. Accordingly, for large g, we may consider $g_{\rm scat}^{(\rm a)} < g$ and simplify Eq. (84) to obtain the following expression for the coefficient of diffusion, which is independent of the frequency, ω, and the wave vector, $\vec{g}$:

$$D_{||}^{(\rm a)} \approx \frac{v_{\rm th}^{(\rm a)}}{g_{\rm scat}^{(\rm a)}} = \left(\frac{k_{\rm B}T}{m_{\rm a}}\right)^{1/2}\frac{1}{g_{\rm scat}^{(\rm a)}}. \tag{87}$$

Equation (87) is the simplest expression for the diffusion coefficient that contains the complete information on collisional dynamics, through $g_{\rm scat}^{(\rm a)}$ as given in Eq. (26) or Eq. (28), involving the constituent molecular species within the system. Let us now make a numerical test for Eq. (87). For a system consisting of potassium ions solvated in water, the value of $g_{\rm scat}^{(\rm K^+)}$, in the low-concentration region (say, at 0.01 M aqueous solution) at 300 K temperature, is approximately equal to $129.524\,{\rm nm}^{-1}$ (see Sec. IV), which, from Eq. (87), implies $D_{||}^{(\rm K^+)} \approx 1.95\times10^{-9}\,{\rm m}^2/{\rm s}$, a value very close to the experiment ($2\times10^{-9}\,{\rm m}^2/{\rm s}$) [1]. Furthermore, if we use the Stokes-Einstein relation, the friction coefficient, γ_f, is obtained from Eq. (87) as follows: $\gamma_f = p_{\rm th}^{(\rm a)}g_{\rm scat}^{(\rm a)} = (m_{\rm a}k_{\rm B}T)^{1/2}g_{\rm scat}^{(\rm a)} \Rightarrow \eta = (\frac{p_{\rm th}^{(\rm a)}}{6\pi R_{\rm H}^{(\rm a)}})g_{\rm scat}^{(\rm a)}$, where η is the viscosity of the medium within which the phenomenon of diffusion occurs and $R_{\rm H}^{(\rm a)}$ is the Stokes (hydrodynamic) radius of the diffusing molecular species. It is important to emphasize here that the quantity $g_{\rm scat}^{(\rm a)}$ appearing in Eq. (87) need not be a constant. As we have discussed in Sec. IV, $g_{\rm scat}^{(\rm a)}$, in a complex molecular environment, may be concentration dependent. We will say more on this later (see Sec. VIII E).

For $\vec{g}=0$, on the other hand, we simplify Eq. (37) by substituting $\vec{g}=0$ for the nonequilibrium distribution function and obtain the expressions for the longitudinal current density and thence the longitudinal conductivity as follows:

$$\vec{J}_{||}^{(\rm a)}(\vec{g}=0,\omega) = Z_{\rm a}e\int_{-\infty}^{\infty}d^3k\frac{\hbar\vec{k}_{||}}{m_{\rm a}}f_{\rm a}^{(\rm neq)}(\vec{g}=0,\vec{k},\omega) \tag{88}$$

$$= \frac{iZ_{\rm a}e}{2\pi m_{\rm a}\tilde{\omega}_{\rm a}}\frac{1}{(2\pi)^2}\iint d^3g'd\omega' \times\left\{\rho_{\rm a}^{(\rm eq)}(-\vec{g}',\omega-\omega')\vec{E}_{\perp}^{(\rm ext)}(\vec{g}',\omega') + \rho_{\rm a}^{(\rm eq)}(\vec{g}',\omega')\vec{E}_{\perp}^{(\rm ext)}(-\vec{g}',\omega-\omega')\right\} \tag{89}$$

$$\approx \frac{iZ_{\rm a}e\langle\rho_{\rm a}^{(\rm eq)}\rangle}{\pi m_{\rm a}\tilde{\omega}_{\rm a}}\vec{E}_{||}^{(\rm ext)}(\vec{g}=0,\omega) \tag{90}$$

$$\Rightarrow \vec{J}_{||}^{(\rm a)}(\vec{g}=0,\omega=0) \approx \frac{Z_{\rm a}e\langle\rho_{\rm a}^{(\rm eq)}\rangle}{\pi m_{\rm a}\sum_{\rm b}\xi_{\rm ab}\langle n_{\rm b}^{(\rm eq)}\rangle} \times\vec{E}_{||}^{(\rm ext)}(\vec{g}=0,\omega=0) \tag{91}$$

$$\Rightarrow \langle\vec{J}_{||}^{(\rm a)}\rangle \approx \frac{Z_{\rm a}e\langle\rho_{\rm a}^{(\rm eq)}\rangle}{\pi m_{\rm a}\sum_{\rm b}\xi_{\rm ab}\langle n_{\rm b}^{(\rm eq)}\rangle}\langle\vec{E}_{||}^{(\rm ext)}\rangle$$

$$\Rightarrow \langle\vec{J}_{||}^{(\rm a)}\rangle = \sigma_{\rm a}\langle\vec{E}_{||}^{(\rm ext)}\rangle, \tag{92}$$

where the average conductivity, $\sigma_{\rm a}$, is the same as that given in Eq. (72). To go from Eq. (89) to Eq. (90), we have used the simplifying expression for the charge density, $\rho_{\rm a}^{(\rm eq)}(\vec{g},\omega) = Z_{\rm a}en_{\rm a}^{(\rm eq)}(\vec{g},\omega)$, as given in Eqs. (35)–(36). As expected, from Eqs. (72) and (92), the average conductivity is the same for the transverse and the longitudinal cases, and therefore we obtain the following general result on the average current density:

$$\langle\vec{J}_{\rm a}\rangle = \sigma_{\rm a}\langle\vec{E}^{(\rm ext)}\rangle. \tag{93}$$

Notably, the situation $\vec{g}=0$ implies the absence of concentration (density) gradient in the system and accordingly the diffusion current simply vanishes. For $\vec{g}\neq0$, on the the other hand, we have, from Eq. (64) and Eq. (78), the following interesting relation between the transverse and longitudinal conductivities:

$$\sigma_{||}^{(\rm a)}(\vec{g},\omega) = \left(\frac{1-x}{1-5x}\right)\sigma_{\perp}^{(\rm a)}(\vec{g},\omega), \tag{94}$$

$$\text{where } x = \frac{k_{\rm B}T}{H_{\rm int}^{(\rm a)}(\vec{g},\omega)} = \frac{g^2k_{\rm B}T}{m_{\rm a}\left(\omega+iv_{\rm th}^{(\rm a)}g_{\rm scat}^{(\rm a)}\right)^2} \tag{95}$$

$$\Rightarrow \sigma_{||}^{(\rm a)}(\vec{g},\omega=0) = \left(\frac{1+y^2}{1+5y^2}\right)\sigma_{\perp}^{(\rm a)}(\vec{g},\omega=0) \quad \left(\text{where } y = g/g_{\rm scat}^{(\rm a)}\right). \tag{96}$$

Equation (96) shows that the longitudinal conductivity, in the limit $g \gg g_{\rm scat}^{(\rm a)}$, converges to the transverse conductivity and they become identical when $g\to0$, as manifested in Eq. (93).

We parenthetically note that the expressions for the transverse and longitudinal conductivities obtained above may also be used to compute the electric permittivity, $\epsilon(\vec{g},\omega)$, and the inverse magnetic permeability, $\zeta(\vec{g},\omega)$, of the system consisting of charged molecular species. Required

relations, following the work of Lindhard [89,90], are as follows: $\epsilon(\vec{g},\omega) = \epsilon_0 - (i/\omega)\sigma_{||}(\vec{g},\omega)$ and $\zeta(\vec{g},\omega) = \zeta_0 + (i\omega/g^2)[\sigma_\perp(\vec{g},\omega) - \sigma_{||}(\vec{g},\omega)]$, where ϵ_0 and ζ_0 respectively are the electric permittivity and the inverse magnetic permeability in vacuum. The magnetic permeability, $\mu(\vec{g},\omega)$, is equal to $1/\zeta(\vec{g},\omega)$.

VI. DIFFUSION AND DISSIPATIVE TRANSPORT

In what follows, we highlight a relation between the charge density, $\rho_a(\vec{g},\omega)$, and the longitudinal current density, $\vec{J}^{(a)}_{\parallel}(\vec{g},\omega)$, which reveals how the notion of charge conservation is modified due to the irreversible nature of the Boltzmann-equation-based ensemble molecular dynamics. Furthermore, as we will see presently, this relation implies a nontrivial extension of the standard diffusion equation, by explicitly incorporating the effect of collisions among various molecular species. To begin, Eqs. (46) and (79) establish the following identity, $\vec{J}^{(a)}_{\parallel}(\vec{g},\omega) = [\tilde{\omega}_a \rho_a^{(neq)}(\vec{g},\omega) + \omega\rho_a^{(eq)}(\vec{g},\omega)]\hat{g}/g$, which implies the following:

$$\rho_a(\vec{g},\omega) = \frac{1}{\tilde{\omega}_a}\left[g J^{(a)}_{\parallel}(\vec{g},\omega) + i v^{(a)}_{th} g^{(a)}_{scat}\rho_a^{(eq)}(\vec{g},\omega)\right] \quad (97)$$

$$= \frac{1}{\omega}\left[g J^{(a)}_{\parallel}(\vec{g},\omega) - i v^{(a)}_{th} g^{(a)}_{scat}\rho_a^{(neq)}(\vec{g},\omega)\right] \quad (98)$$

$$\Rightarrow \left(\frac{\partial}{\partial t} + v^{(a)}_{th} g^{(a)}_{scat}\right)\rho_a(\vec{r},t) + \vec{\nabla}\cdot\vec{J}^{(a)}(\vec{r},t) = v^{(a)}_{th} g^{(a)}_{scat}\rho_a^{(eq)}(\vec{r},t). \quad (99)$$

Notably, $g^{(a)}_{scat} = 0$, when there are no interactions among molecular species (see Sec. IV), in which case Eq. (99) represents the conservation of charge density for molecular species a. Also, the thermal speed, $v^{(a)}_{th} = \sqrt{k_B T/m_a}$, at zero temperature is manifestly zero, in which circumstance the strict conservation of charge trivially prevails. In a sense, then, Eq. (99) reveals a necessary conceptual modification to the notion of charge conservation for the irreversible transport processes wherein the molecular scattering provides a mechanism of dissipation, consistent with the viewpoint of Van Hove [80]. Next, we note that $\vec{J}^{(a)}(\vec{r},t)$ in Eq. (99) consists of contributions both from the conduction and the diffusion current and they are easily separated, if so required. For example, if we identify $\vec{J}^{(a)}(\vec{r},t)$ with the diffusion current and use a constitutive relation $\vec{J}^{(a)}(\vec{r},t) = -D^{(a)}_{||}\vec{\nabla}\rho_a(\vec{r},t)$ (Fick's law) with $D^{(a)}_{||}$ as the diffusion coefficient [2], then we obtain, using Eq. (87), a generalized diffusion equation as follows:

$$\left(\hbar\frac{\partial}{\partial t} - \frac{\hbar^2}{2m^{(a)}_{eff}}\nabla^2 + u^{(a)}_{eff}\right)\rho_a(\vec{r},t) = u^{(a)}_{eff}\rho_a^{(eq)}(\vec{r},t), \quad (100)$$

where $m^{(a)}_{eff} = (\hbar g^{(a)}_{scat}/2)\sqrt{m_a/(k_B T)}$ may be interpreted as the temperature- and collision-induced *effective mass* of the diffusing molecules. It is worth remembering here that the actual inertial mass of the diffusing molecules also plays the necessary mechanical role in quantum collision dynamics, which gives the operational meaning to the collision operator as given, for example, in Eq. (23). Similarly, $u^{(a)}_{eff} = \hbar g^{(a)}_{scat}\sqrt{k_B T/m_a}$ may be conceived as the temperature-dependent effective "potential energy", originating from the scattering events in the system. Notably, Eq. (100) is analogous to the Schrödinger equation (in Euclidean time) with a source term, and therefore $m^{(a)}_{eff}$ and $u^{(a)}_{eff}$ may as well be treated as the free model parameters. In any event, with Eq. (26) as a model for $g^{(a)}_{scat}$, Eq. (100) offers a well-defined equation of motion to study diffusive transport processes, wherein collisional events are expected to be important, such as those frequently encountered within the crowded environment of the biological cells and complex molecular liquids. As a further generalization, we just note that $m^{(a)}_{eff}$ and $u^{(a)}_{eff}$ would, in general, be dependent on the number density of molecular species a, and this is particularly expected to be the case when there are position-dependent variations in the complexity of the surrounding molecular environment. In such a situation, $m^{(a)}_{eff}$ and $u^{(a)}_{eff}$ would depend on the position variable, implicitly through the density, $\rho_a(\vec{r},t)$. This also effectively renders the temperature to be a locally defined quantity in the position space, thus giving a useful avenue to study the effects of temperature gradient, *if any*, present in the system. Equation (100) may accordingly be further generalized, leading to a nonlinear theory of diffusive transport. To obtain a numerical perspective, let us now, as an example, evaluate $m^{(a)}_{eff}$ and $u^{(a)}_{eff}$ for 0.01 M aqueous solution of potassium ion at 300 K, for which $g^{(a)}_{scat}$ has been approximately evaluated to be $0.129524307 \times 10^{12}$ m^{-1} (see Sec. IV). The final results are as follows: $m^{(K^+)}_{eff} \approx 16.28356$ amu and $u^{(K^+)}_{eff} \approx 2.0777$ kJ/mole $= 21.5336$ mV. This is revealing. What this actually means is that the diffusive transport of potassium ion (mass = 39.0983 amu) in the aqueous environment may be viewed as a deterministic dynamics of the ensemble of quasipotassium ions (each with a mass ≈16 amu, at 300 K), immersed within an effective temperature-dependent one-body potential barrier (≈2 kJ/mole at 300 K); that is, as if an effective voltage (≈21.5 mV at 300 K) has been impressed on the ensemble of quasipotassium ions, each of mass 16 amu. We thus obtain a purely mechanical interpretation of diffusive transport processes in nature. This is important, for the diffusive motion is frequently conceived as a stochastic phenomenon, wherein the diffusing species perform a random walk movement. In summary, Eq. (99) and its generalizations, in conjunction with a detailed (and more realistic) constitutive relations connecting the current density and its various causes, may be used to study drift and diffusion processes in those varieties of physical and biological systems, for which the microscopic scattering events matter.

VII. SELF-ENERGY: FIELD RENORMALIZATION

Using Eqs. (17) and (97), we now compute the longitudinal electric field, $\vec{E}^{(a)}_{||}(\vec{g},\omega)$, solely due to the charged molecular species a, as follows:

$$\vec{E}^{(a)}_{||}(\vec{g},\omega) = -\frac{i\hat{g}}{g\epsilon}\rho_a(\vec{g},\omega) = \frac{1}{\epsilon\tilde{\omega}_a}\left[\frac{\hat{g}}{g}\left(\sum_b \xi_{ab}\langle n_b^{(eq)}\rangle\right)\rho_a^{(eq)}(\vec{g},\omega) - i\vec{J}^{(a)}_{\parallel}(\vec{g},\omega)\right], \quad (101)$$

where $J_{\parallel}^{(a)}(\vec{g},\omega)$ is as given in Eq. (74) or (79). As $\omega \to 0$, $\tilde{\omega}_a \to \sum_b \xi_{ab}\langle n_b^{(eq)}\rangle$ and therefore the situation when $\vec{g} \to 0$ we have, from Eq. (101), the following expression for the average longitudinal electric field:

$$\langle \vec{E}_{\parallel}^{(a)} \rangle = -\frac{1}{\epsilon}\left[\frac{\langle \vec{J}_{\parallel}^{(a)} \rangle}{\sum_b \xi_{ab}\langle n_b^{(eq)}\rangle} + i\langle \rho_a^{(eq)}\rangle \left(\lim_{g\to 0} \frac{1}{g} \right) \langle \hat{E}_{\parallel}^{(a)} \rangle \right], \tag{102}$$

where $\langle \hat{E}_{\parallel}^{(a)} \rangle$ is the unit vector and $\langle \vec{J}_{\parallel}^{(a)} \rangle$ is as given in Eq. (92). To understand the meaning of the limiting process in the second term on the right-hand side of Eq. (102), we use Eqs. (92) and (102) to evaluate, using the Poynting theorem [86], the average energy per molecule of species a, associated with the longitudinal electric field, $\langle \vec{E}_{\parallel}^{(a)} \rangle$, as follows:

$$\begin{aligned} \langle W_{\parallel}^{(a)} \rangle &= \frac{\epsilon}{2\langle n_a \rangle} |\langle \vec{E}_{\parallel}^{(a)} \rangle|^2 \\ &= \frac{\epsilon}{2\langle n_a^{(eq)} \rangle} |\langle \vec{E}_{\parallel}^{(a)} \rangle|^2 = \frac{Z_a e}{2\epsilon} \langle \rho_a^{(eq)} \rangle \\ &\quad \times \left[\left(\frac{Z_a e \langle \vec{E}_{\parallel}^{(ext)} \rangle}{\pi m_a \left(\sum_b \xi_{ab} \langle n_b^{(eq)} \rangle \right)^2} \right)^2 + \left(\lim_{g\to 0} \left[\frac{1}{g} \right] \right)^2 \right]. \end{aligned} \tag{103}$$

Evidently, the second term on the right-hand side of Eq. (103) stands for the average self-energy of an individual molecule of species a, which is formally infinity, as we expect. Suppose, now, that the individual molecule of species a is not a point charge, but it is a sphere of a finite radius. We then compute, from classical electrodynamics, the self-energy of the sphere of finite total charge, $Z_a e$, with radius, R_a, and equate with the self-energy term in Eq. (103), to obtain the following meaning for the limiting process in Eq. (103):

$$\begin{aligned} \frac{(Z_a e)^2}{2\epsilon} \langle n_a^{(eq)} \rangle \left[\lim_{g\to 0} \left(\frac{1}{g} \right) \right]^2 &= \lim_{R_a \to 0} \frac{3(Z_a e)^2}{20\pi\epsilon R_a} \Rightarrow \lim_{g\to 0} \left(\frac{1}{g} \right) \\ &= \lim_{R_a \to 0} \left(\frac{3}{10\pi \langle n_a^{(eq)} \rangle R_a} \right)^{1/2}. \end{aligned} \tag{104}$$

Equation (104) provides a well-defined meaning to the self-energy (formally, an infinity) in terms of the radius, R_a, of the individual molecular species. We will say more on the physical estimate of R_a later (see Sec. VIII B). In a sense, then, Eq. (104) introduces a characteristic length scale associated with the problem at hand. With Eq. (104), Eq. (103) may be written as follows:

$$\langle W_{\parallel}^{(a)} \rangle = \frac{\langle n_a^{(eq)} \rangle}{2\pi^2 \epsilon} \left(Z_a e L_a^{(EM)} \right)^2 \tag{105}$$

$$\text{where} \quad L_a^{(EM)} = \left[\left(\frac{Z_a e |\langle \vec{E}_{\parallel}^{(ext)} \rangle|}{\pi m_a \left(\sum_b \xi_{ab} \langle n_b^{(eq)} \rangle \right)^2} \right)^2 + \left(\frac{3}{10\pi \langle n_a^{(eq)} \rangle R_a} \right) \right]^{1/2}. \tag{106}$$

Finally, with Eqs. (92), (102), and (104), the renormalized form of the average longitudinal electric field arising due to the ensemble of molecular species a may be written as follows:

$$\begin{aligned} \langle \vec{E}_{\parallel}^{(a)} \rangle = -\frac{1}{\epsilon} \Bigg[&\frac{\langle n_a^{(eq)} \rangle}{\pi m_a} \left(\frac{Z_a e}{\sum_b \xi_{ab} \langle n_b^{(eq)} \rangle} \right)^2 \langle \vec{E}_{\parallel}^{(ext)} \rangle \\ &+ i Z_a e \left(\frac{3\langle n_a^{(eq)} \rangle}{10\pi R_a} \right)^{1/2} \langle \hat{E}_{\parallel}^{(a)} \rangle \Bigg]. \end{aligned} \tag{107}$$

To be consistent, using Eq. (17), the transverse electric field, $\vec{E}_{\perp}^{(a)}(\vec{g},\omega)$, due to the charged molecular species a, is given as follows:

$$\vec{E}_{\perp}^{(a)}(\vec{g},\omega) = \frac{i\tilde{\omega}_a \mu}{g^2 - \mu\epsilon\tilde{\omega}_a^2} \vec{J}_{\perp}^{(a)}(\vec{g},\omega) \tag{108}$$

$$\begin{aligned} \Rightarrow \langle \vec{E}_{\perp}^{(a)} \rangle &= -\frac{\langle \vec{J}_{\perp}^{(a)} \rangle}{\epsilon \sum_b \xi_{ab} \langle n_b^{(eq)} \rangle} \\ &= -\frac{\langle n_a^{(eq)} \rangle}{\pi\epsilon m_a} \left(\frac{Z_a e}{\sum_b \xi_{ab} \langle n_b^{(eq)} \rangle} \right)^2 \langle \vec{E}_{\perp}^{(ext)} \rangle, \end{aligned} \tag{109}$$

where $\vec{J}_{\perp}^{(a)}(\vec{g},\omega)$ is as given in Eqs. (61)–(67). To arrive at Eq. (109), we have used Eq. (72) for $\langle \vec{J}_{\perp}^{(a)} \rangle$. Thus, the total average renormalized electric field, $\langle \vec{E}^{(a)} \rangle = \langle \vec{E}_{\parallel}^{(a)} \rangle + \langle \vec{E}_{\perp}^{(a)} \rangle$, arising due to molecular species a is given as follows:

$$\begin{aligned} \langle \vec{E}^{(a)} \rangle = -\frac{1}{\epsilon} \Bigg[&\frac{\langle n_a^{(eq)} \rangle}{\pi k_B T} \left(\frac{Z_a e}{g_{scat}^{(a)}} \right)^2 \langle \vec{E}^{(ext)} \rangle \\ &+ i Z_a e \left(\frac{3\langle n_a^{(eq)} \rangle}{10\pi R_a} \right)^{1/2} \langle \hat{E}_{\parallel}^{(a)} \rangle \Bigg]. \end{aligned} \tag{110}$$

Next, using Eq. (18), the magnetic field, $\vec{B}_{\perp}^{(a)}(\vec{g},\omega)$, due to the charged molecular species a, is obtained as follows:

$$\begin{aligned} \vec{B}_{\perp}^{(a)}(\vec{g},\omega) &= \frac{ig\mu}{g^2 - \mu\epsilon\tilde{\omega}_a^2} \hat{g} \times \vec{J}_{\perp}^{(a)}(\vec{g},\omega) \\ \Rightarrow \langle \vec{B}^{(a)} \rangle &= \langle \vec{B}_{\parallel}^{(a)} \rangle + \langle \vec{B}_{\perp}^{(a)} \rangle = 0, \end{aligned} \tag{111}$$

where $\vec{J}_{\perp}^{(a)}(\vec{g},\omega)$ is as given in Eqs. (61)–(67).

VIII. APPLICATIONS

In what follows, we use results from Secs. V–VII and obtain analytical expressions for the chemical potential, activity coefficient, conductance, and the current-voltage curve.

A. Chemical potential

For electromagnetic processes, from classical thermodynamics, the change in the free energy for molecular species a, at a given temperature, volume, pressure, and number of particles, is equal to the total electromagnetic work done on the complete ensemble of molecular species a. Since the change in the chemical potential, $\Delta\mu_a$, is, by definition, equal to the change in the free energy per mole, we have $\Delta\mu_a = N_A\langle w_a \rangle$, where N_A is the Avogadro number and $\langle w_a \rangle$ is the average

electromagnetic work done per charged molecular entity, of species a. By definition, then,

$$\langle w_{\rm a}\rangle = \frac{u^{(\rm a)}_{\rm tot}}{n^{(\rm a)}_{\rm tot}} - u^{(\rm self)}_{\rm a}, \tag{112}$$

$$\text{with } n^{(\rm a)}_{\rm tot} = \iint d^3 r dt n_{\rm a}(\vec{r},t) = (2\pi)^2 [n_{\rm a}(\vec{g},\omega)]_{\substack{\vec{g}\to 0\\ \omega\to 0}}, \tag{113}$$

$$u^{(\rm a)}_{\rm tot} = \iint d^3 r dt u_{\rm a}(\vec{r},t) = (2\pi)^2 [u_{\rm a}(\vec{g},\omega)]_{\substack{\vec{g}\to 0\\ \omega\to 0}}. \tag{114}$$

In Eqs. (113) and (114), $n_{\rm a}(\vec{r},t)$ is the number density of molecular species a at the space-time point $(\vec{r},t)$ and $u_{\rm a}(\vec{r},t)$ is the space-time energy density belonging to the molecular species a, which, according to the Poynting theorem [86], is as given below:

$$u_\alpha(\vec{r},t) = \frac{\epsilon}{2}\sum_\beta \mathrm{Re}(\vec{E}^{(\alpha)}(\vec{r},t)\cdot[\vec{E}^{(\beta)}(\vec{r},t)]^* + c_{\rm med}\vec{B}^{(\alpha)}(\vec{r},t)\cdot[c_{\rm med}\vec{B}^{(\beta)}(\vec{r},t)]^*) \tag{115}$$

$$\Rightarrow [u_\alpha(\vec{g},\omega)]_{\substack{\vec{g}\to 0\\ \omega\to 0}} = \frac{\epsilon}{2}\sum_\beta \mathrm{Re}\iint d^3 g_1 d\omega_1 (\vec{E}^{(\alpha)}(\vec{g}_1,\omega_1)\cdot[\vec{E}^{(\beta)}(\vec{g}_1,\omega_1)]^* + c_{\rm med}\vec{B}^{(\alpha)}(\vec{g}_1,\omega_1)\cdot[c_{\rm med}\vec{B}^{(\beta)}(\vec{g}_1,\omega_1)]^*), \tag{116}$$

where ϵ is the dielectric constant of the medium and $c_{\rm med} = 1/\sqrt{\mu\epsilon}$ is the speed of the electromagnetic wave within the medium. $\vec{E}^{(\alpha)}(\vec{r},t)/\vec{B}^{(\alpha)}(\vec{r},t)$ is the renormalized electric-magnetic field (see Sec. VII) arising due to the ensemble of charged molecular species α. The summation in Eqs. (115) and (116) runs over the variety of charged molecular species present in the system. The quantity $u^{(\rm self)}_{\rm a}$ in Eq. (112) stands for the self-energy of the species a (see Sec. VII). Notably, Eq. (115) implies the following expression for the total work done, $u(t)$, in assembling the complete system of charged molecular species at its configuration at the time t:

$$u(t) = \frac{\epsilon}{2}\int d^3 r(|\vec{E}_{\rm tot}(\vec{r},t)|^2 + |c_{\rm med}\vec{B}_{\rm tot}(\vec{r},t)|^2) \tag{117}$$

$$\text{with}\quad \vec{E}_{\rm tot}(\vec{r},t) = \sum_\alpha \vec{E}^{(\alpha)}(\vec{r},t) \text{and} \vec{B}_{\rm tot}(\vec{r},t) = \sum_\alpha \vec{B}^{(\alpha)}(\vec{r},t). \tag{118}$$

Now, Eqs. (112)–(116) yield the following expression for the chemical potential for the ensemble of charged molecular species a:

$$\Delta\mu_{\rm a} = N_{\rm A}\iint d^3 g d\omega \mu_{\rm a}(\vec{g},\omega) \tag{119}$$

$$\text{with}\quad \mu_\alpha(\vec{g},\omega) = \frac{\epsilon}{2(2\pi)^2[n_\alpha(\vec{g},\omega)]_{\substack{\vec{g}\to 0\\ \omega\to 0}}} \times \sum_\beta \mathrm{Re}(\vec{E}^{(\alpha)}(\vec{g},\omega)\cdot[\vec{E}^{(\beta)}(\vec{g},\omega)]^* + c_{\rm med}\vec{B}^{(\alpha)}(\vec{g},\omega)\cdot[c_{\rm med}\vec{B}^{(\beta)}(\vec{g},\omega)]^*) - u^{(\rm self)}_\alpha, \tag{120}$$

where $\mu_\alpha(\vec{g},\omega)$ is the local chemical potential density in the frequency–wave vector space. If we approximate the integral in Eq. (119) by letting $\mu_\alpha(\vec{g},\omega)$ be equal to $(2\pi)^2\langle\mu_\alpha\rangle\delta(\vec{g})\delta(\omega)$, then we have the following expression for the chemical potential:

$$\Delta\mu_{\rm a} \approx N_{\rm A}\frac{[\mu_{\rm a}(\vec{g},\omega)]_{\substack{\vec{g}\to 0\\ \omega\to 0}}}{[n_{\rm a}(\vec{g},\omega)]_{\substack{\vec{g}\to 0\\ \omega\to 0}}} = N_{\rm A}\frac{\langle\mu_{\rm a}\rangle}{\langle n_{\rm a}\rangle} = N_{\rm A}\frac{\langle\mu_{\rm a}\rangle}{\langle n^{(\rm eq)}_{\rm a}\rangle} \tag{121}$$

$$\text{with}\quad \langle\mu_{\rm a}\rangle = \frac{\epsilon}{2}\sum_\beta \mathrm{Re}\big[\langle\vec{E}^{(\rm a)}\rangle\cdot\langle\vec{E}^{(\beta)}\rangle^* + c^2_{\rm med}\langle\vec{B}^{(\rm a)}\rangle\cdot\langle\vec{B}^{(\beta)}\rangle^*\big] - u^{(\rm self)}_{\rm a}. \tag{122}$$

Finally, we substitute the renormalized expressions for the average electric and magnetic fields from Eqs. (110) and (111) in Eqs. (121) and (122) to obtain the chemical potential for molecular species a, the final expression of which is as given below:

$$\Delta\mu_\alpha = N_{\rm A}\sum_\beta\big(\Gamma_\alpha\Gamma_\beta\langle n^{(\rm eq)}_\beta\rangle + \Delta_{\alpha\beta}\big), \tag{123}$$

$$\text{where}\quad \Gamma_{\rm a} = \frac{(2\epsilon)^{-1/2}}{\pi m_{\rm a}}\left(\frac{Z_{\rm a}e}{\sum_{\rm j}\xi_{\rm aj}\langle n^{(\rm eq)}_{\rm j}\rangle}\right)^2 |\langle\vec{E}^{(\rm ext)}\rangle| \tag{124}$$

$$\text{and}\quad \Delta_{\rm ab} = \frac{3Z_{\rm a}Z_{\rm b}e^2}{20\pi\epsilon}\frac{(1-\delta_{\rm ab})}{\sqrt{R_{\rm a}R_{\rm b}}}\left(\frac{\langle n^{(\rm eq)}_{\rm b}\rangle}{\langle n^{(\rm eq)}_{\rm a}\rangle}\right)^{1/2}. \tag{125}$$

B. Activity coefficient

Using the chemical potential from Sec. VIII A, we obtain the activity coefficient, γ_α, as $\ln\gamma_\alpha = (k_{\rm B}T)^{-1}\sum_\beta(\Gamma_\alpha\Gamma_\beta\langle n^{(\rm eq)}_\beta\rangle + \Delta_{\alpha\beta})$. The mean ionic activity coefficient, γ, for the electrolyte of the type, $\mathrm{A}^{(Z_{\rm a})}_{\nu_{\rm a}}\mathrm{B}^{(Z_{\rm b})}_{\nu_{\rm b}}\mathrm{C}^{(Z_{\rm c})}_{\nu_{\rm c}}\ldots$, is $\prod_\beta[(\gamma_\beta)^{\nu_\beta}]^{1/\nu}(\nu = \sum_\beta\nu_\beta)$, which implies the following expression for $\ln\gamma$:

$$\ln\gamma = \frac{1}{\nu k_{\rm B}T}\sum_\alpha\sum_\beta \nu_\alpha\big(\Gamma_\alpha\Gamma_\beta\langle n^{(\rm eq)}_\beta\rangle + \Delta_{\alpha\beta}\big). \tag{126}$$

Let us now consider, as an example, the case of a z:z-valent electrolyte (KCl, say) within the confinement of a solvent (H_2O, say), in which case we have $Z_{\rm a} = z = -Z_{\rm b}$ and $\langle n^{(\rm eq)}_{\rm a}\rangle = \langle n^{(\rm eq)}_{\rm b}\rangle = \langle n\rangle$. Furthermore, if there is no external field acting on the electrolyte solution, $\langle\vec{E}^{(\rm ext)}\rangle$ may be equated to the average electric field, $\langle\vec{E}^{(\rm s)}\rangle$, arising due to the polarization of the solvent, $\langle\vec{E}^{(\rm s)}\rangle$. The activity coefficient, γ, from Eq. (126), then takes the following form:

$$\ln\gamma = L_0\kappa^{(\rm ab)}_{\rm eff} = L_0\big(\kappa^{(\rm ab)}_{\rm Dynamic} - \kappa^{(\rm ab)}_{\rm Singular}\big), \tag{127}$$

where $\kappa^{(\rm ab)}_{\rm Dynamic} = (1/\pi\langle n\rangle^3)[ze\langle\vec{E}^{(\rm s)}\rangle(m^{-1}_{\rm a}(\xi_{\rm aa}+\xi_{\rm ab})^{-2} + m^{-1}_{\rm b}(\xi_{\rm ba}+\xi_{\rm bb})^{-2})]^2 = (I/\pi)[e\langle\vec{E}^{(\rm s)}\rangle(m^{-1}_{\rm a}(\omega_{\rm aa}+\omega_{\rm ab})^{-2} + m^{-1}_{\rm b}(\omega_{\rm ba}+\omega_{\rm bb})^{-2})]^2$, $\kappa^{(\rm ab)}_{\rm Singular} = 1/R^{(\rm ab)}_{\rm av} = (3/5)(R_{\rm a}R_{\rm b})^{-1/2}$, $L_0 = z^2e^2/(4\pi\epsilon k_{\rm B}T) = z^2e^2/(4\pi\epsilon_0\epsilon_r k_{\rm B}T) = \frac{z^2}{\epsilon_{\rm r}}\times 55.700319\,\mathrm{nm}$

at 300 K and ϵ_r is the relative dielectric constant of the medium. $R_{\rm av}^{\rm (ab)}$ is the average length associated with the physical nature of the Coulomb singularity, involving the charged molecular species a and b, embedded within a given molecular environment and $\xi_{\alpha\beta}$ is as given in Eqs. (23). The symbol I stands for the ionic strength of the electrolyte and $\omega_{\alpha\beta}$ is interpreted as the scattering frequency involving the ionic species α and β. As Eq. (127) shows, the behavior of $\ln\gamma$ as a function of the electrolyte concentration, $\langle n\rangle$, is universal and it is fully determined by the effective wave number, $\kappa_{\rm eff}^{\rm (ab)}$, which is here given as the difference of $\kappa_{\rm Dynamic}^{\rm (ab)}$ and $\kappa_{\rm Singular}^{\rm (ab)}$, available to the system, wherein L_0 sets the fundamental length scale (temperature dependent) associated with the system. Notably, given the set of approximations involved in the present study, the expression for $\kappa_{\rm Dynamic}^{\rm (ab)}$ as obtained here may be taken as tentative, albeit a fairly accurate, estimate. Improved expressions for $\kappa_{\rm Dynamic}^{\rm (ab)}$ that reflect the presence of complex environment in a more realistic manner may be obtained by considering, on physical ground, the quantity, $\xi_{\rm ab}$, which is related to the scattering length (a quantum mechanical object), $s_{\rm ab}$, through Eq. (23), as dependent on the electrolyte concentration, $\langle n\rangle$ (cf. Sec. IV). Now, there are several conclusions we may draw from Eqs. (127), as we delineate below.

First, $\kappa_{\rm Singular}^{\rm (ab)}$ arises from the length scale, $R_{\rm av}^{\rm (ab)}$, of the singularity, which, at a given finite temperature and concentration, $\langle n\rangle$, is expected to be smaller than other length scales of the problem at hand. That is, in a normal physical situation, $\kappa_{\rm Singular}^{\rm (ab)}$ is expected to be larger than $\kappa_{\rm Dynamic}^{\rm (ab)}$, which implies $\ln\gamma$ to be a negative number. As a consequence, γ, from Eq. (127), would be less than unity as one usually expects. However, γ would assume a value which is greater than unity only in the situation when there exists at least one physical length scale within the system which, at some given temperature and the electrolyte concentration, happens to be smaller than the length scale of the singularity; that is, $\kappa_{\rm Singular}^{\rm (ab)} < \kappa_{\rm Dynamic}^{\rm (ab)}$, and this situation is not completely unrealistic and it may as well be found in nature, albeit not so frequently.

Next, interestingly, the limiting situation, $\kappa_{\rm Dynamic}^{\rm (ab)} \to \kappa_{\rm Singular}^{\rm (ab)}$, *inter alia*, gives a physical meaning to the concept of the *ideal solution*, a notion frequently used in the studies of electrolytes in physical and biological sciences. Before we discuss this situation in detail, let us first understand the nature of the quantity, $\kappa_{\rm Dynamic}^{\rm (ab)}$. The scattering length, $s_{\rm ab}$, which, through Eqs. (23), defines $\xi_{\rm ab}$, and therefore $\kappa_{\rm Dynamic}^{\rm (ab)}$, is here synonymous with the range of the effective hard sphere potential (approximately, a distance of closest approach) involving the molecular pair (a, b), and this distance, as we have discussed earlier in Sec. IV A, is, in general, a function [a decreasing one, cf. Eq. (29)] of the electrolyte concentration, $\langle n\rangle$, arising due to the phenomenon of solvation or caging that may occur, particularly in complex molecular environments. As a consequence, the dependence of $\kappa_{\rm Dynamic}^{\rm (ab)}$ on $\langle n\rangle$ comes from two interlinked sources: (a) an explicit power law such as $1/\langle n\rangle^3$, as obtained here, and (b) an implicit dependence through the quantity, $\xi_{\rm ab}$. The implicit dependence, as we will see later, contains rich chemistry and it allows us to go beyond the DHO phenomenology on electrolyte solutions.

Let us now consider the limiting case $\kappa_{\rm Dynamic}^{\rm (ab)} \to \kappa_{\rm Singular}^{\rm (ab)}$ first in the simplest situation when $s_{\rm ab}$ does not depend on the concentration of the electrolyte solution. At a given finite temperature, the nontrivial situation $\kappa_{\rm Dynamic}^{\rm (ab)} - \kappa_{\rm Singular}^{\rm (ab)} = 0$ would occur at a critical concentration, $\langle n\rangle = \langle n_{\rm c}\rangle$, which, from Eq. (127), is given as follows: $\langle n_{\rm c}\rangle = (R_{\rm av}^{\rm (ab)}/\pi)^{1/3}[ze\langle\vec{E}^{\rm (s)}\rangle \times (m_{\rm a}^{-1}(\xi_{\rm aa}+\xi_{\rm ab})^{-2} + m_{\rm b}^{-1}(\xi_{\rm ba}+\xi_{\rm bb})^{-2})]^{2/3}$. At $\langle n\rangle = \langle n_{\rm c}\rangle$, we have $\ln\gamma = 0 \Rightarrow \gamma = 1$, which is the standard definition for the *ideal solution* in equilibrium thermodynamics. One may thus fruitfully use the limiting process $\kappa_{\rm Dynamic}^{\rm (ab)} \to \kappa_{\rm Singular}^{\rm (ab)}$ as an operational definition for the *ideal electrolyte solution*. Now, the *ideal solution* in thermodynamics is frequently conceptualized as an entity, which is practically synonymous to the physically noninteracting many-body systems. And, therefore, the critical concentration, $\langle n_{\rm c}\rangle$, may also be likened to that concentration which defines the notion of *infinite dilution* in equilibrium thermodynamics. We will say more on this later.

We now consider the limiting case $\kappa_{\rm Dynamic}^{\rm (ab)} \to \kappa_{\rm Singular}^{\rm (ab)}$ for the situations when $s_{\rm ab}$ does depend on the concentration of the electrolyte solution. At a given temperature, here, the circumstance $\kappa_{\rm Dynamic}^{\rm (ab)} - \kappa_{\rm Singular}^{\rm (ab)} = 0$ would, in general, yield a number of roots, $\langle n\rangle = \langle n_j\rangle$, the exact nature of which is critically dependent on the detailed analytical form of the dependence of $s_{\rm ab}$, and thereby $\xi_{\rm ab}$, on $\langle n\rangle$. Each root, $\langle n_j\rangle$, in any event, corresponds to $\ln\gamma \to 0 \Rightarrow \gamma \to 1$. In such a situation, the smallest (magnitude) root may be taken as the critical concentration, $\langle n_{\rm c}\rangle$, that defines the *ideal electrolyte solution*. In actual practice, however, there may exist only one nontrivial root, defining the critical concentration, $\langle n_{\rm c}\rangle$. Before we proceed further, let us now examine the behavior of $\kappa_{\rm Dynamic}^{\rm (ab)}$ as a function of $\langle n\rangle$. From Eq. (127), we obtain the following expression for the slope of the $\ln\gamma$ versus $\langle n\rangle$ curve,

$$\frac{\partial}{\partial\langle n\rangle}\ln\gamma \approx \frac{8L_0}{\langle n\rangle}(\theta_{\rm av}-\theta_c)\kappa_{\rm Dynamic}^{\rm (ab)}, \tag{128}$$

where $\theta_c = 3/8$ and the dimensionless (positive-valued) quantity, $\theta_{\rm av}$, is as defined in Eq. (29). Again, given the set of approximations involved in the present study, the numerical value for θ_c may be taken as tentative, though a realistic estimate for practical purposes. Now, $s_{\rm ab}$ is only weakly dependent on $\langle n\rangle$, which would particularly be the case in the regime of low electrolyte concentrations ($\langle n\rangle \to 0$). In such a situation, $s_{\rm ab}$ is, as discussed in Sec. IV A, expectedly large, and therefore the ratio $\langle n\rangle/s_{\rm ab}$ is vanishingly small. That means, from Eq. (29), we will have a vanishingly small $\theta_{\rm av}$, assuming the derivative, $ds_{\rm ab}/d\langle n\rangle$, does not fluctuate too strongly in the low-concentration regime; that implies the slope of the $\ln\gamma$ versus $\langle n\rangle$ curve, from Eq. (128), would yield a negative value. The conclusion therefore is that $\ln\gamma$, in the low-concentration regime, would decrease with the increase of $\langle n\rangle$. This behavior is fully consistent with the prediction of the Debye-Hückel (DH) phenomenology on strong electrolytes as well as numerous experimental observations [2]. Furthermore, this situation would continue to hold for finite values of $\theta_{\rm av}$, as Eq. (128) reveals, until it reaches the critical point, $\theta_{\rm av} = \theta_c$. We designate the range, $0 \leqslant \theta_{\rm av} < \theta_c$, as belonging to the *DH regime*, whereas the range $\theta_{\rm av} > \theta_c$, which is not covered by the original DH phenomenology, as the *non-DH regime* wherein the slope of the $\ln\gamma$ versus $\langle n\rangle$ curve becomes positive

and consequently $\ln\gamma$ starts increasing with the increase of the $\langle n\rangle$. Notably, the existence of the *non-DH regime* is an experimentally verified fact [2]. Next, the extremum point, $\theta_{\rm av}=\theta_c$, at which the slope of the $\ln\gamma$ versus $\langle n\rangle$ curve is zero, may, in general, occur for a number of concentration values, $\langle n\rangle=\langle n_j\rangle$, the exact nature of which would be determined by the detailed mathematical behavior of $\theta_{\rm av}$ as a function of $\langle n\rangle$. As an example, $\theta_{\rm av}$, as defined in Eq. (29), may as well happen to be a function of $\langle n\rangle$, that oscillates (with decaying amplitude) around $\theta_{\rm av}=\theta_c$, in which circumstance $\ln\gamma$ as a function of $\langle n\rangle$, according to Eq. (127), would, in general, exhibit an oscillatory behavior, with $\langle n_j\rangle$ being the locations of various extrema. A tentative physical picture for such a scenario is that the charged molecular species constituting the electrolyte tend to alternate between the state of solvation or caging and the state of desolvation or decaging, as we systematically increase the electrolyte concentration. This prediction is open to experimental verifications. If, on the other hand, the extremum condition, $\theta_{\rm av}=\theta_c$, is satisfied for only one nontrivial concentration value, $\langle n_c\rangle$, then the $\ln\gamma$ versus $\langle n\rangle$ curve, beyond $\langle n\rangle=\langle n_c\rangle$, would possess a positive slope and exhibit a nonoscillatory behavior; that is, $\ln\gamma$, beyond $\langle n\rangle=\langle n_c\rangle$, would simply increase as the $\langle n\rangle$ increases, possibly reaching an asymptotic value at high electrolyte concentrations. Notably, it is the nonoscillatory behavior of the $\ln\gamma$ versus $\langle n\rangle$ curve that is frequently encountered in experiments [2]. A schematic description of the behavior of $\ln\gamma$ as a function of $\langle n\rangle$, at a given temperature, for various possible physical scenarios is presented in Fig. 1 (all curves a, b, c, and d).

We now discuss the meaning of the DH limiting law, which is known to hold at low electrolyte concentrations, within the precinct of the present theoretical elaboration, as summarized in Eq. (127). The DH limiting law, that connects $\ln\gamma_{\rm DH}$ and the ionic strength, I, is stated as follows: $\ln\gamma_{\rm DH}=-A_{\rm DH}I^{1/2}$, where $A_{\rm DH}$ is a constant. To proceed, let us consider the expression for $\kappa^{\rm (ab)}_{\rm Dynamic}$ in terms of the ionic strength I and the scattering frequency, $\omega_{\alpha\beta}$, as given in Eq. (127). In order to have a realistic description that takes cognizance of the complex molecular environment, we may consider $\omega_{\alpha\beta}$ to be a function of I. In fact, on physical ground, we expect $\omega_{\alpha\beta}$ to increase with the increase of I. This behavior of the scattering frequency is also seen in the complete thermal equilibrium situation, wherein the total number of collisions per unit volume and per unit time between a pair of molecular species is known to be proportional to the product of their equilibrium number densities [75]. In any event, then, the dependence of $\kappa^{\rm (ab)}_{\rm Dynamic}$ on I consists of two factors: (a) an explicit power law (proportional to I, that is) as obtained here and (b) an implicit dependence through $\omega_{\alpha\beta}$, with the slope, $d\omega_{\alpha\beta}/dI$, being positive definite. Now, using Eq. (127), we evaluate the slope of the $\ln\gamma$ versus $\sqrt{I}$ curve as follows:

$$\frac{d\ln\gamma}{dI^{1/2}}=(\psi_c-\psi_{\rm av})\frac{8L_0}{I^{1/2}}\kappa^{\rm (ab)}_{\rm Dynamic} \tag{129}$$

$$\text{with}\quad \left(\frac{d\omega_{\alpha\beta}}{dI}\right)\approx\frac{\omega_{\alpha\beta}}{I}\psi_{\rm av}, \tag{130}$$

where $\psi_c=1/4$. Notably, Eq. (130), like Eq. (29), is an independent postulate that defines a form for $(d\omega_{\alpha\beta}/dI)$ through the dimensionless quantity, $\psi_{\rm av}$, which may depend on the ionic strength, I. In order to recover the DH limiting law, we must have, from Eq. (129), the following identity at low ionic strengths: $\psi_{\rm av}=\psi_c+(A_{\rm DH}/8L_0)(I^{1/2}/\kappa^{\rm (ab)}_{\rm Dynamic})$, which provides a dynamical interpretation of the DH limiting law. Accordingly, then, Eq. (130) yields the following expression for $\omega_{\alpha\beta}$:

$$\omega_{\alpha\beta}=\omega^{(0)}_{\alpha\beta}\left[\psi_c\ln I+\frac{A_{\rm DH}}{8L_0}\int\frac{dI}{I^{1/2}\kappa^{\rm (ab)}_{\rm Dynamic}}\right], \tag{131}$$

where $\omega^{(0)}_{\alpha\beta}$ is the constant of integration. Equation (131) provides a definite condition on $\omega_{\alpha\beta}$ that is necessary for the DH limiting law to hold. To gain further insight in the region of low ionic strengths, we may approximately evaluate the integral in Eq. (131) as follows. As Eqs. (127) and (128) reveal, $\kappa^{\rm (ab)}_{\rm Dynamic}$, in the low-concentration region ($\theta_{\rm av}<\theta_c$), decreases with the increase of $\langle n\rangle$ (and wherefore the ionic strength, I), and, therefore, let us introduce a power law dependence for $\kappa^{\rm (ab)}_{\rm Dynamic}$ as follows: $\kappa^{\rm (ab)}_{\rm Dynamic}=\tilde{\kappa}^{\rm (ab)}_{\rm Dynamic}I^{-\delta}(\delta>0)$, which, from Eq. (131), yields $\omega_{\alpha\beta}=\omega^{(0)}_{\alpha\beta}[\psi_c\ln I+(A_{\rm DH}/4L_0)(I^{\delta+1/2}/2\delta+1)\tilde{\kappa}^{\rm (ab)}_{\rm Dynamic}]$, an explicit expression for the scattering frequency, necessary for the DH limiting law to exactly hold.

Finally, to obtain a numerical insight into the present theory, let us use the simplified expressions in Eqs. (127) to compute the activity coefficient for potassium chloride (KCl) in aqueous solution at 300 K. For simplicity, we use the scattering length (a distance of closest approach), $s_{\rm k^+Cl^-}$, to be 0.267 nm, which is a standard estimate for the equilibrium separation of potassium and chloride ions. We consider the surrounding water molecules to form a dipolar solvent medium, which generates an electric field. To make an estimate for the electric field arising due to the aqueous medium, we use a simple expression from classical electrostatics as follows: $\langle E^{\rm (s)}\rangle=\langle E^{\rm (H_2O)}\rangle=\mu^{\rm (H_2O)}/(\epsilon_0\epsilon_{\rm H_2O}\langle n_{\rm H_2O}\rangle)$, where $\mu^{\rm (H_2O)}=1.8546$ D, $\langle n_{\rm H_2O}\rangle=3.3311508\times10^{28}$ m^{-3}, and $\epsilon_{\rm H_2O}=80$ respectively stand for the dipole moment, number density, and the relative permittivity of water, and ϵ_0 is the permittivity of the free space. Accordingly, we estimate, $\langle E^{\rm (H_2O)}\rangle\approx2.909\times10^8$ V/m. For further simplicity, we here consider collisions only between K^+ and Cl^- ions; that is, we ignore the effects of K^+-K^+ and Cl^--Cl^- collisions, and also assume that the scattering length, $s_{\rm K^+-Cl^-}$, does not depend on the electrolyte (KCl) concentration. Equation (127) then finally yields $\kappa^{\rm (KCl)}_{\rm Dynamic}=0.164\times10^{17}$ m^{-1}, 0.164×10^{14} m^{-1}, and 0.164×10^{11} m^{-1} respectively for 0.01, 0.1, and 1 molar KCl solutions in water. If this system is to behave normally (that is, $\ln\gamma$ for KCl in Eq. (127) is to remain less than zero) then $\kappa^{\rm (KCl)}_{\rm Singular}$ must be greater than 0.164×10^{14} m^{-1} for 0.1 M aqueous KCl solution, for example. In contrast, let us evaluate $\kappa^{\rm (KCl)}_{\rm Singular}$ using the ionic radius for K^+ ($R_{\rm K^+}=0.138$ nm) and Cl^- ($R_{\rm Cl^-}=0.181$ nm) ions, which yields $\kappa^{\rm (KCl)}_{\rm Singular}\approx0.38\times10^{10}$ m^{-1}, a value that is smaller than $\kappa^{\rm (KCl)}_{\rm Dynamic}$ for 0.1 M aqueous KCl solution. This indicates, from Eq. (127), a positive value for $\ln\gamma_{\rm KCl}$, which is possibly not a physically acceptable scenario. This then implies that the typical ionic radii for the charged species tend to overestimate the physical length scale of the singularity,

associated with the longitudinal part of the electric field; equivalently, the use of ionic radii possibly underestimates the self-energy, which is otherwise infinite for point particles (cf. Sec. VII). The conclusion then is that the idea of introducing a simple correction for the finite size of ions in terms of their ionic radii, which have frequently been used in earlier theoretical works [2], to improve upon the activity coefficients and equivalent conductivities for strong electrolytes in the high concentration regime, may not always be sufficient to faithfully capture the essence of physical reality. In fact, within the high-concentration regime, s_{ab}, which through Eqs. (23) and (127) defines $\kappa^{(\mathrm{KCl})}_{\mathrm{Dynamic}}$, is itself expectedly concentration dependent, which renders the subject of strong electrolytes even more subtle in physical conception and the experimental realization.

C. Molar and equivalent conductivity

We here obtain a simple expression for the molar conductivity of electrolytes, which is expected to be useful for a variety of electrochemical studies on chemical and biological systems. We consider a z:z-valent electrolyte, embedded within an explicit solvent. That is, the charge number of the molecular species satisfy $Z_a = z = -Z_b$ and the corresponding number densities are abbreviated as follows: $\langle n_a^{(eq)}\rangle = \langle n_b^{(eq)}\rangle = \langle n\rangle$. The number density of the solvent molecules is denoted by the symbol, $\langle n_s^{(eq)}\rangle$. The equivalent conductivity, Λ, of the electrolyte is defined as follows: $\Lambda = \Lambda_m/z = \sigma/(cz) = N_A\sigma/(z\langle n\rangle)$, where N_A is the Avogadro number, Λ_m is the molar conductivity, σ stands for the (specific) conductivity of the electrolyte, and $c = \langle n\rangle/N_A$ is the concentration of the electrolyte. The total conductivity, σ, is defined as the sum of the conductivities of all charged molecular species present in the system, which we compute using Eqs. (72) and (92). Finally, Λ_m, takes the following form:

$$\begin{aligned}\Lambda_m &= \frac{N_A}{\langle n\rangle}\sum_\alpha \sigma_\alpha \\ &= \frac{N_A}{\pi}\frac{(ze)^2}{(k_BT)^{1/2}}\left(\frac{1}{(m_a)^{1/2}g^{(a)}_{scat}} + \frac{1}{(m_b)^{1/2}g^{(b)}_{scat}}\right).\end{aligned} \tag{132}$$

To obtain a simple numerical test for Eq. (132), let us consider the molar conductivity of 0.01 M solution of potassium chloride (KCl) in water at 300 K temperature. To compute an approximate value for $g^{(Cl^-)}_{scat}$ form Eq. (26), we obtain an estimate for $s_{Cl^-H_2O}$ from *ab initio* quantum chemical studies [91,92], which is about 0.25 nm. Accordingly, then, Eq. (26) yields $g^{(Cl^-)}_{scat} = 0.29\times10^{12}\ \mathrm{m}^{-1}$. Using an *ab inito* quantum chemical estimate of 0.165 nm for $s_{K^+H_2O}$, the value for $g^{(K^+)}_{scat}$, from Eq. (26), is equal to $0.13\times10^{12}\ \mathrm{m}^{-1}$, as obtained earlier (see Sec. IV A). Finally, Λ_m from Eq. (132), is 3.41×10^{-3} S m^2 mol^{-1}, which compares well with the experimental value [93], 15.46×10^{-3} S m^2 mol^{-1}. Accordingly, the specific conductivity of aqueous KCl, σ_{KCl}, is 3.41×10^{-2} S m^{-1} (theory) / 15.46×10^{-2} S m^{-1} (expt) [93]. The apparent discrepancy between the present theoretical estimate and the experiment values for the specific conductivity is attributed to the approximate evaluation of $g^{(a)}_{scat}$, which is possibly an overestimate here.

To get physical insight, let us, for simplicity, assume that the scattering length, s_{as}, involving the solvent molecule s does not depend on the electrolyte concentration, $\langle n\rangle$, and evaluate, using Eqs. (33) and (132), the slope of the Λ_m versus $\langle n\rangle$ curve as follows: $\partial\Lambda_m/\partial\langle n\rangle = C\times(\theta_{av}-\theta_c)$, where $C>0$, $\theta_c = 1/2$ and θ_{av} is as given in Eq. (29). This is revealing because it shows that the dimensionless (positive-valued) quantity θ_{av}, which measures the average fluctuation of the scattering length in a given complex molecular environment, plays the role of a tuning variable. For example, when $\theta_{av}<\theta_c$ the slope is negative and therefore Λ_m decreases with the increase of $\langle n\rangle$, which is fully consistent with the DHO phenomenology. This is the low-concentration region, which we here designate as the *Onsager regime*. Next, Λ_m reaches a minimum at $\theta_{av}=\theta_c$. For $\theta_{av}>\theta_c$, the slope is positive and therefore Λ_m increases with the increase of $\langle n\rangle$. This is the high-concentration region, which is not covered under the original DHO phenomenology and therefore we designate this as the *non-Onsager regime*. Notably, the location of the critical point, $\theta_{av}=\theta_c=1/2$, here is only an estimate, which should be improved by more elaborate computations. In general, as we have discussed in Sec. IV A, the system may possess a number of critical points, which are to be determined as the solutions of Eq. (29). In such a situation, the Λ_m versus $\langle n\rangle$ curve would exhibit an oscillatory behavior, superimposed over a decaying amplitude. Physically, this situation may be attributed to the existence of dynamical association and dissociation of electrolyte as one changes the electrolyte concentration. A schematic plot of the Λ_m versus $\langle n\rangle$ curve for various physical scenarios is shown in Fig. 1 (curve d).

D. Current-voltage characteristics

Using results of Sec. V, we here obtain a simple expression for the current-voltage curve, useful to study various ion-transport processes in biological channels and pumps. The component of the current vector along the jth direction of an orthogonal coordinate system, $I^{(a)}_j(\vec{g},\omega)$, belonging to molecular species a is defined as follows: $I^{(a)}_j(\vec{g},\omega) = S_j J^{(a)}_j(\vec{g},\omega)$, where $J^{(a)}_j(\vec{g},\omega)$ is the current density along the jth direction. S_j stands for the cross-sectional area perpendicular to the direction of the jth unit vector. Using Eqs. (64), (76), and (78) to the leading order, we obtain the following expression for the current:

$$\begin{aligned}&I^{(a)}_j(\vec{g},\omega) \\ &= S_j Z_a e\Bigg\{(1+x^2)\frac{g_j}{g^2}(\tilde{\omega}_a-\omega)n^{(eq)}_a(\vec{g},\omega) \\ &\quad+\frac{Z_a e}{2}\frac{\langle n^{(eq)}_a\rangle}{m_a\tilde{\omega}_a}\sum_l\left[\left(5-\frac{1}{x^2}\right)\delta_{jl}-\frac{3g_jg_l}{g^2}\left(1-\frac{1}{x^2}\right)\right] \\ &\quad\times\left[g_l\phi^{(ext)}(\vec{g},\omega)-\omega A^{(ext)}_l(\vec{g},\omega)\right]\Bigg\}\end{aligned} \tag{133}$$

$$\Rightarrow\ \langle\vec{I}_a\rangle = S_{\vec{I}_a}\frac{(Z_ae)^2\langle n^{(eq)}_a\rangle}{\pi(m_ak_BT)^{1/2}g^{(a)}_{scat}}\langle\vec{E}^{(ext)}\rangle, \tag{134}$$

where $x = v_{\rm th}^{(a)} g/\tilde{\omega}_a$ and g_j is the jth Cartesian component of $\vec{g}$. $\phi^{(\rm ext)}(\vec{g},\omega)$ and $A_l^{(\rm ext)}(\vec{g},\omega)$ are the externally applied scalar and the lth component of the vector potential respectively. In Eq. (133), the first term is the diffusion current whereas the second term is the conduction current, arising due to the external 4-potentials. In Eq. (134), $S_{\vec{I}_a}$ is the cross-sectional area, perpendicular to the direction of the current, $\vec{I}_a$.

In order to transform Eq. (134) to the potential (voltage) form, we now consider, as a specific example, the circular cylindrical geometry with coordinate variables as (R,ϕ,z) and imagine that the transport of ions is taking place in the z direction, in which circumstance, we may take $\langle \vec{E}^{(\rm ext)} \rangle = \Delta\phi_{\rm ext}/L$, where $\Delta\phi_{\rm ext}$ is the average potential difference (external voltage) across the cylinder of length, L. Accordingly, Eq. (134) yields the following expression for the average current-voltage curve:

$$\langle I_a \rangle = G_a \Delta\phi_{\rm ext} = \left|T_{\rm scat}^{(a)}\right|^2 \frac{e^2}{\hbar} \Delta\phi_{\rm ext} \tag{135}$$

$$\text{where} \quad \left|T_{\rm scat}^{(a)}\right|^2 = \left[\frac{(Z_a R)^2 \langle n_a^{(\rm eq)} \rangle}{k_{\rm th}^{(a)} g_{\rm scat}^{(a)} L}\right] \tag{136}$$

$$\approx \frac{1}{8\sqrt{\pi}} \frac{(Z_a R)^2}{L} \left\{ \sum_\beta \left(1 + \frac{m_a}{m_\beta}\right) \frac{\langle n_\beta^{(\rm eq)} \rangle}{\langle n_a^{(\rm eq)} \rangle} \frac{[1 - {}_1F_1(2;1/2;-\xi_0)]}{k_{\rm th}^{(a\beta)}} \right\}^{-1}, \tag{137}$$

where $\langle I_a \rangle$ is the average current and G_a is the conductance for molecular species a. The summation in Eq. (137) spans over all charged molecular species present in the system. To pass from Eq. (136) to Eq. (69), we have used Eqs. (23)–(26) for $g_{\rm scat}^{(a)}$. To examine the numerical performance of Eq. (136), we here consider the flow of potassium ions, embedded in the aqueous environment (0.1 M aqueous solution), along a circular cylindrical channel (length, $L = 4$ nm, and the cross-sectional radius, $R = 0.2$ nm) at 300 K. Also, we use an approximate value for $g_{\rm scat}^{(K^+)}$, which is equal to $0.1295 \times 10^{12}\ {\rm m}^{-1}$ (cf. Sec. IV A). Accordingly, the conductance, G_{K^+}, from Eq. (135), is 7.28 pS. As we have noted in Sec. VIII C, the value of $g_{\rm scat}^{(K^+)}$ used here is possibly an overestimate and therefore we expect 7.28 pS for G_{K^+} to be an underestimate here. Notably, most ion channels in biological cells have a conductance in the range of 1 to 150 pS [4]. This gives us confidence in the present theoretical formulation on the characteristics of the current-voltage curve.

Interestingly, the expression for G_a, in Eq. (135), generalizes the work, originally due to Landauer and subsequently extended by others [32–34], that views conductance as the transmission processes. Following this viewpoint, the coefficient of transmission, $|T_{\rm scat}^{(a)}|^2$, here is, *inter alia*, intimately related to the collisional events, through $s_{a\beta}$. Thus, Eqs. (135)–(137) present a nontrivial unification of quantum scattering with the conduction processes, which may be fruitfully used to study a variety of chemical, biophysical, and mesoscopic systems. To gain a qualitative insight on the current-voltage curve, let us recall (Sec. IV A) that $s_{a\beta}$ may potentially depend upon the density, $\langle n_a^{(\rm eq)} \rangle$, as well as the external voltage, $\Delta\phi_{\rm ext}$. Let us examine the behavior of the current, $\langle I_a \rangle$, as a function of $\langle n_a^{(\rm eq)} \rangle$. Using Eqs. (29) and (135)–(137), we obtain the slope of the $\langle I_a \rangle$ versus $\langle n_a^{(\rm eq)} \rangle$ curve as follows: $d\langle I_a \rangle / d\langle n_a^{(\rm eq)} \rangle \approx (1 + 2\theta_{\rm av}) \langle I_a \rangle / \langle n_a^{(\rm eq)} \rangle$ where the dimensionless $\theta_{\rm av}$, which defines the derivative $ds_{a\beta}/d\langle n_a^{(\rm eq)} \rangle$ through Eq. (29), is a positive number (see Sec. IV A), meaning the $\langle I_a \rangle$ versus $\langle n_a^{(\rm eq)} \rangle$ curve possesses no extremum. From Eqs. (135)–(137), G_a is also a positive definite quantity. That means that the current will always increases with the increase of concentration of molecular species a, as we normally expect. Next, let us examine the behavior of the current, $\langle I_a \rangle$, as a function of the external voltage, $\Delta\phi_{\rm ext}$, at a given concentration. Using Eqs. (29) and (135)–(137), we compute the slope of the $\langle I_a \rangle$ versus $\Delta\phi_{\rm ext}$ curve as follows:

$$\frac{d\langle I_a \rangle}{d(\Delta\phi_{\rm ext})} \approx 2(\theta_{\rm av} + \theta_c) G_a \quad (\text{where } \theta_c = 1/2), \tag{138}$$

where θ_c is a number, independent of the external voltage, $\Delta\phi_{\rm ext}$. Notably, as we have discussed in Sec. IV A, the dimensional quantity $\theta_{\rm av}$ in Eq. (138), which defines the derivative $ds_{a\beta}/d(\Delta\phi_{\rm ext})$, like Eq. (29), may now admit all possible values (negative, zero, and positive). In fact, as we will see presently, $\theta_{\rm av}$ is never positive. Now, let us consider Eq. (135), which is essentially a statement of the well-known Ohm's law, provided the conductance, G_a, is simply a constant; that is, G_a does not depend on the external voltage, $\Delta\phi_{\rm ext}$. In the Ohmic conduction regime (the low-voltage regime, that is), therefore, if G_a happens to be independent of the voltage, so must be the case with ξ_0 and thence the scattering length, s_{ab}, as Eqs. (23) and (135)–(137) clearly reveal, which, in turn, implies, from Eq. (29), that $\theta_{\rm av}$ must be identically zero. Next, the expression for the slope in Eq. (138) indicates the existence of three distinct regions for the current-voltage curve, as schematically shown in Fig. 2. In region I, where the magnitude of the current increases with the increase of the voltage, we have $\theta_{\rm av} > -\theta_c$, from Eq. (138). That means that region I, which includes the pure Ohmic regime, is bounded by the inequality, $-\theta_c < \theta_{\rm av} \leqslant 0$. We designate region I as the *normal conduction regime*. In region II, which is here characterized by the condition $\theta_{\rm av} = -\theta_c$, the current no longer depends on the external voltage. We designate this as the *saturation current regime*, within which the scattering length, s_{ab}, as Eq. (29) reveals, simply exhibits a power-law behavior; that is, $s_{ab} \propto (\Delta\phi_{\rm ext})^{\theta_c}$. This power-law behavior of s_{ab} may thus be taken as a defining characteristic for the existence of the

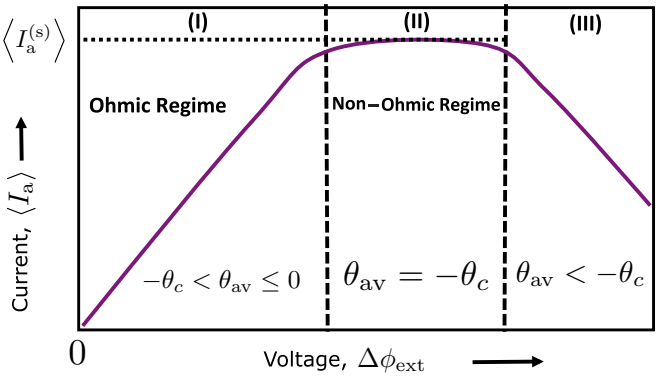

FIG. 2. A schematic representation for the current-voltage characteristics. The behavior of θ_{av} in Eq. (138), which encodes the average variation of the scattering length with the external voltage, clearly differentiates the saturation regime (the middle region) from the normal (the left region) and the anomalous (the right region) conduction regimes.

saturation current regime in the system. Region III is defined by the inequality $\theta_{av} < -\theta_c$, which implies that the slope in Eq. (138) is negative and therefore the current will decrease with the increase of the external voltage. We designate this as the *anomalous conduction regime*. The scattering length, s_{ab}, would increase with the increase of the external voltage in both regions I and III, but the increase in region I, because of the inequality, $-\theta_c < \theta_{av} \leqslant 0$, will be slower, whereas the increase in region III, because of the inequality, $\theta_{av} < -\theta_c$, will be faster, in comparison to the power law behavior of region II. As s_{ab} measures the distance of closest approach for the pair of species involved in collision, the three regimes of the current-voltage curve, as discussed above and schematically displayed in Fig. 2, unfolds the possible physical mechanisms for the role of the external voltage on the microscopic dynamics of charged molecular species, eventually leading to a rich variety of conduction scenarios. The existence of the anomalous conduction region may be rationalized for the circumstance when the dynamic charged molecular species undergo nontrivial chemical reactions forming a variety of long-lived molecular species, thereby decreasing the population of charged species available for the conduction processes. The presence of the *anomalous conduction* region is a prediction here, which may be verified in experiments.

E. Concentration dependence of the diffusion coefficient

We here address the following question: How does the coefficient of diffusion behave as a function of the concentration of the diffusing molecular species in a complex molecular environment? This is important because the diffusive transport processes are frequently found to be anomalous, meaning they deviate from the standard linear law for the mean square displacement versus time curve due to Einstein, Smoluchowski, and others [85,94–100], particularly for the molecular ions within the crowded environment of biological cells. To obtain a qualitative understanding, let us, for simplicity, consider Eq. (87), which expresses the diffusion coefficient in terms of $g_{scat}^{(a)}$, which may be a function of the concentration of the molecular species a, particularly when there is a complex molecular environment present in the system (cf. Sec. IV A). We now use Eqs. (26)–(29) and (87) and evaluate the slope of the $D_{||}^{(a)}$ versus $\langle n_a^{(eq)} \rangle$ curve as follows:

$$\frac{dD_{||}^{(a)}}{d\langle n_a^{(eq)} \rangle} \approx \frac{2D_{||}^{(a)}}{\langle n_a^{(eq)} \rangle}(\theta_{av} - \theta_c), \tag{139}$$

where $\theta_c = 32\sqrt{\pi}(s_{aa})^2 \langle n_a^{(eq)} \rangle / g_{scat}^{(a)}$ and θ_{av}, a positive and dimensionless number, approximately defines the derivative of the scattering length with respect to the density of molecular species a, as shown in Eq. (29). It is also clear from Eqs. (26) and (139) that the critical value θ_c is a positive and dimensionless number. Furthermore, as we have argued elsewhere [see the discussion after Eq. (128)], θ_{av} is expected to be vanishingly small in the low-concentration region. Equation (139) then implies that the slope would be negative in the low-concentration region, until θ_{av} reaches the critical value θ_c. That means the coefficient of diffusion, $D_{||}^{(a)}$, in the low-concentration region, is expected to decrease as we increase $\langle n_a^{(eq)} \rangle$. Beyond the critical point, $\theta_{av} = \theta_c$, lies the high-concentration region, wherein $D_{||}^{(a)}$ is expected to increase with the increase of $\langle n_a^{(eq)} \rangle$. In fact, the critical point $\theta_{av} = \theta_c$ may be satisfied by a number of densities, $\langle n_a^{(eq)} \rangle = \langle n_a^{(j)} \rangle$, of the molecular species a, in which case the $D_{||}^{(a)}$ versus $\langle n_a^{(eq)} \rangle$ curve would manifest an oscillatory behavior, as schematically shown in Fig. 1 (curve d). This oscillatory behavior may be attributed to the possibility of continuous transitions of molecular species from the state of solvation and caging to the state of desolvation and decaging, as we increase the density of the molecular species. The oscillation in the $D_{||}^{(a)}$ versus $\langle n_a^{(eq)} \rangle$ curve, as we have predicted here, may be verified in experiments. Such behavior of the coefficient of diffusion would provide necessary physical reasons for the existence of anomalous diffusion phenomena [85,96–100] that one frequently encounters in biological systems, in particular.

IX. CONCLUSIONS

We have presented a complete theoretical framework to understand a wide variety of experiments on equilibrium and nonequilibrium behaviors of charge carriers, which are embedded within a complex molecular atmosphere, such as the solvents and the crowded environment of biological cells, in the presence of electromagnetic potentials. Present elaboration transcends the well-known Debye-Hückel-Onsager and Poisson-Nernst-Planck phenomenologies and their variants, which have frequently been used to study strong electrolytes and the flow of ions in transmembrane protein channels in biological cells. We now briefly outline how the present theoretical framework may be further extended and utilized to study the equilibrium and the transport processes, involving charged molecular species, in chemical and biophysical sciences. An important outcome of the present discourse, as discussed in Sec. VI, is a conceptually new theoretical setting that manifestly is cognizant of microscopic molecular scattering events, for diffusive transport, and which generalizes the traditional framework of the diffusion equation. This may be fruitfully used to rationalize and understand the anomalies in

diffusive transport, frequently encountered, particularly within the environment of biological cells. As yet another important development, the present work has established a nontrivial connection between the current-voltage characteristics of ions in a complex molecular environment and the Landauer's viewpoint on electrical conduction in mesoscopic systems (see Sec. VIII D), which may be used to conceptually link important physical ideas across the apparently two disjoint fields of research in physical science and beyond. The present theoretical structure may be further extended and enriched in a number of ways. First, we have considered only binary quantum elastic collisions, involving a simplified mathematical form for the intermolecular potential, to obtain a mathematically tractable yet physically realistic expression for the Boltzmann collision operator. A better description for quantum collisions is certainly warranted here. Next, the present mathematical solution of the Boltzmann transport equation is necessarily approximate. A rigourous and mathematically enriched approach to the Boltzmann equation would be needed to improve upon the necessary quantitative predictions. The electromagnetic properties of charged entities constituting the system as well as the complex molecular environment have been studied here by assuming them to be point particles. In specific situations, for a more realistic physical description, the present work may be updated by incorporating, for example, an elaborate multipole expansion of the electromagnetic fields. The present work may also be extended to obtain an analytical expression for frequency- and wave-vector-dependent viscosity and study the phenomenon of glass transitions. Furthermore, the present work has not explicitly explored the role, *if any*, of quantum statistics. For example, quantum statistics for indistinguishable molecular objects, particularly at low temperatures, have important consequences, which may unravel yet unexplored regimes of new phenomena involving charged molecular species in biological settings. An investigation along this direction should be enriching. We will present such studies in future publications.

ACKNOWLEDGMENTS

Sathiya Mahakrishnan acknowledges Indian Institute of Technology Madras, India, for fellowship. Subrata Chakraborty acknowledges the financial support from Centre for Industrial Consultancy and Sponsored Research, Indian Institute of Technology Madras, India under Grant No. ICS1617831RFIEMAHS/R47522.

[1] R. Phillips, J. Kondev, J. Theriot, and H. G. Garcia, *Physical Biology of the Cell*, 2nd ed. (Garland Science, London and New York, 2013).
[2] J. O. Bockris and A. K. N. Reddy, *Modern Electrochemistry*, 2nd ed., Vol. 1 (Plenum Press, New York, 1998).
[3] E. Gouaux and R. MacKinnon, Science **310**, 1461 (2005).
[4] B. Hille, *Ion Channels of Excitable Membranes*, 3rd ed. (Sinauer Associates, Sunderland, MA, 2001).
[5] C. Koch, *Biophysics of Computation: Information Processing in Single Neurons* (Oxford University Press, New York, 1999).
[6] T. M. Squires and S. R. Quake, Rev. Mod. Phys. **77**, 977 (2005).
[7] R. B. Schoch, J. Han, and P. Renaud, Rev. Mod. Phys. **80**, 839 (2008).
[8] P. C. Bressloff and J. M. Newby, Rev. Mod. Phys. **85**, 135 (2013).
[9] Y. Imry, *Introduction to Mesoscopic Physics*, 2nd ed. (Oxford University Press, New York, 2009).
[10] P. Debye and E. Hückel, Phys. Z. **24**, 305 (1923).
[11] P. Debye and H. Falkenhagen, Phys. Z. **29**, 401 (1928).
[12] L. Onsager and R. M. Fuoss, J. Phys. Chem. **36**, 2689 (1932).
[13] R. M. Fuoss and L. Onsager, Proc. Natl. Acad. Sci. USA **41**, 274 (1955).
[14] F. Filippo Accascina, R. L. Kay, and C. A. Kraus, Proc. Natl. Acad. Sci. USA **45**, 804 (1959).
[15] R. M. Fuoss, J. Solution Chem. **7**, 771 (1978).
[16] M.-S. Chen and L. Onsager, J. Phys. Chem. **81**, 2017 (1977).
[17] W. Nernst, Z. Phys. Chem. **2U**, 613 (1888).
[18] W. Nernst, Z. Phys. Chem. **4U**, 129 (1889).
[19] M. Planck, Ann. Phys. **276**, 561 (1890).
[20] M. Planck, Ann. Phys. **275**, 161 (1890).
[21] J. E. Mayer, J. Chem. Phys. **18**, 1426 (1950).
[22] J. G. Kirkwood and F. P. Buff, J. Chem. Phys. **19**, 774 (1951).
[23] J. C. Poirier, J. Chem. Phys. **21**, 965 (1953).
[24] J. C. Rasaiah and H. L. Friedman, J. Chem. Phys. **48**, 2742 (1968).
[25] P. Drude, Ann. Phys. **306**, 566 (1900).
[26] P. Drude, Ann. Phys. **308**, 369 (1900).
[27] A. Sommerfeld, Z. Phys. **47**, 1 (1928).
[28] F. Bloch, Z. Phys. **52**, 555 (1929).
[29] R. Kubo, J. Phys. Soc. Jap. **12**, 570 (1957).
[30] W. Kohn and J. M. Luttinger, Phys. Rev. **108**, 590 (1957).
[31] J. M. Luttinger and W. Kohn, Phys. Rev. **109**, 1892 (1958).
[32] A. Kamenev and W. Kohn, Phys. Rev. B **63**, 155304 (2001).
[33] R. Landauer, IBM J. Res. Dev. **1**, 223 (1957).
[34] Y. Imry and R. Landauer, Rev. Mod. Phys. **71**, S306 (1999).
[35] L. D. Landau, Sov. Phys. JETP **3**, 920 (1957).
[36] J.-P. Hansen and I. R. McDonald, *Theory of Simple Liquids*, 3rd ed. (Academic Press, London, 2006).
[37] D. L. Bowers and E. E. Salpeter, Phys. Rev. **119**, 1180 (1960).
[38] G. Trefalt, S. H. Behrens, and M. Borkovec, Langmuir **32**, 380 (2016), and references therein.
[39] D. Fraenkel, J. Chem. Theory Comput. **11**, 178 (2015), and references therein.
[40] I. Valent, P. Petrovič, P. Neogrády, I. Schreiber, and M. Marek, J. Phys. Chem. B **117**, 14283 (2013).
[41] J. Forsman, J. Phys. Chem. B **108**, 9236 (2004).
[42] Z. Abbas, M. Gunnarsson, E. Ahlberg, and S. Nordholm, J. Phys. Chem. B **106**, 1403 (2002).
[43] R. Kjellander and D. Mitchell, Chem. Phys. Lett. **200**, 76 (1992).
[44] M. Z. Bazant, K. Thornton, and A. Ajdari, Phys. Rev. E **70**, 021506 (2004).
[45] B. D. Storey and M. Z. Bazant, Phys. Rev. E **86**, 056303 (2012).
[46] B. Honig and A. Nicholls, Science **268**, 1144 (2005).
[47] H. Hwang, G. C. Schatz, and M. A. Ratner, J. Phys. Chem. B **110**, 6999 (2006).

[48] A. Syganow and E. von Kitzing, J. Phys. Chem. **99**, 12030 (1995).
[49] A. Syganow and E. von Kitzing, Eur. Biophys. J. **28**, 393 (1999).
[50] B. P. Lee and M. E. Fisher, Phys. Rev. Lett. **76**, 2906 (1996).
[51] G. Moy, B. Corry, S. Kuyucak, and S.-H. Chung, Biophys. J. **78**, 2349 (2000).
[52] B. Corry, S. Kuyucak, and S.-H. Chung, Biophys. J. **78**, 2364 (2000).
[53] O. Bernard, W. Kunz, P. Turq, and L. Blum, J. Phys. Chem. **96**, 3833 (1992).
[54] P. Graf, M. G. Kurnikova, R. D. Coalson, and A. Nitzan, J. Phys. Chem. B **108**, 2006 (2004).
[55] D. G. Luchinsky, R. Tindjong, I. Kaufman, P. V. E. McClintock, and R. S. Eisenberg, Phys. Rev. E **80**, 021925 (2009), and references therein.
[56] R. S. Eisenberg, Adv. Chem. Phys. **148**, 77 (2011).
[57] Q. Zheng and G.-W. Wei, J. Chem. Phys. **134**, 194101 (2011).
[58] P. W. Wolynes, Ann. Rev. Phys. Chem. **31**, 345 (1980).
[59] P. Attard, Phys. Rev. E **48**, 3604 (1993).
[60] T. Xiao and X. Song, J. Chem. Phys. **135**, 104104 (2011).
[61] R. I. Slavchov, J. Chem. Phys. **140**, 164510 (2014).
[62] B. Maribo-Mogensen, G. M. Kontogeorgis, and K. Thomsen, Ind. Eng. Chem. Res. **51**, 5353 (2012).
[63] J. Janecek and R. R. Netz, J. Chem. Phys. **130**, 074502 (2009).
[64] M. M. Kohonen, M. E. Karaman, and R. M. Pashley, Langmuir **16**, 5749 (2000).
[65] A. Chandra, R. Biswas, and B. Bagchi, J. Am. Chem. Soc. **121**, 4082 (1999).
[66] A. Chandra and B. Bagchi, J. Chem. Phys. **110**, 10024 (1999).
[67] A. Chandra and B. Bagchi, J. Phys. Chem. B **104**, 9067 (2000), and references therein.
[68] S. Roy, S. Yashonath, and B. Bagchi, J. Chem. Phys. **142**, 124502 (2015), and references therein.
[69] J.-F. Dufreche, O. Bernard, S. Durand-Vidal, and P. Turq, J. Phys. Chem. B **109**, 9873 (2005), and references therein.
[70] C. C. Aburto and G. Nägele, J. Chem. Phys. **139**, 134109 (2013).
[71] H. M. Villullas and E. R. Gonzalez, J. Phys. Chem. B **109**, 9166 (2005).
[72] A. A. Lee, S. Kondrat, D. Vella, and A. Goriely, Phys. Rev. Lett. **115**, 106101 (2015).
[73] S. D. Fried, L.-P. Wang, S. G. Boxer, P. Ren, and V. S. Pande, J. Phys. Chem. B **117**, 16236 (2013).
[74] S. G. Brush, *Kinetic Theory: The Chapman-Enskog Solution of the Transport Equation for Moderately Dense Gases* (Pergamon Press, Oxford, 1972), pp. 3–283; this monograph contains the English translation of the original papers of David Enskog, beside a historical survey on this subject .
[75] S. Chapman and T. G. Cowling, *The Mathematical Theory of Non-uniform Gases*, 3rd ed. (Cambridge University Press, Cambridge, UK, 1995).
[76] H. Grad, Comm. Pure Appl. Math. **2**, 331 (1949).
[77] L. D. Landau, Sov. Phys. JETP **5**, 101 (1957).
[78] A. A. Abrikosov and I. M. Khalatnikov, Rep. Prog. Phys. **22**, 329 (1959).
[79] A. A. Abrikosov, *Fundamentals of the Theory of Metals* (North-Holland, Amsterdam, The Netherlands, 1988).
[80] L. Van Hove, Physica (Amsterdam) **23**, 441 (1957).
[81] J. Keilson and J. E. Storer, Q. Appl. Math. **10**, 243 (1952).
[82] A. M. Smith, A. A. Lee, and S. Perkin, J. Phys. Chem. Lett. **7**, 2157 (2016).
[83] D. J. Kouri and D. K. Hoffman, in *Multiparticle Quantum Scattering with Applications to Nuclear, Atomic, and Molecular Physics*, edited by D. G. Truhlar and B. Simon (Springer-Verlag, New York, 1997), pp. 19–101.
[84] J. J. Sakurai, *Modern Quantum Mechanics* (Addison-Wesley, New York, 1995), Chap. 7.
[85] S. Mahakrishnan, S. Chakraborty, and A. Vijay, J. Phys. Chem. B **120**, 9608 (2016).
[86] J. A. Stratton, *Electromagnetic Theory* (John Wiley & Sons, Inc., Hoboken, NJ, 2007).
[87] O. Borodin, R. L. Bell, Y. Li, D. Bedrov, and G. D. Smith, Chem. Phys. Lett. **336**, 292 (2001).
[88] M. Carrillo-Tripp, H. Saint-Martin, and I. Ortega-Blake, J. Chem. Phys. **118**, 7062 (2003).
[89] J. Lindhard, Dan. Mat . Fys. Medd. **28**, 8 (1954).
[90] M. Renuka and A. Vijay, J. Phys. Chem. C **118**, 7018 (2014).
[91] J. B. Foresman and C. L. Brooks, J. Chem. Phys. **87**, 5892 (1987).
[92] J. M. Heuft and E. J. Meijer, J. Chem. Phys. **119**, 11788 (2003).
[93] *CRC Handbook of Chemistry and Physics*, 97th ed., edited by W. M. Haynes (CRC Press, NJ, 2016), Sec. 5, p. 74.
[94] A. Einstein, *Investigations on the Theory of the Brownian Movement* (Dover, New York, 1956).
[95] M. von Smoluchowski, Ann. Phys. **326**, 756 (1906).
[96] S. Liu, L. Bönig, J. Detch, and H. Metiu, Phys. Rev. Lett. **74**, 4495 (1995).
[97] R. Metzler, J.-H. Jeon, A. G. Cherstvy, and E. Barkai, Phys. Chem. Chem. Phys. **16**, 24128 (2014).
[98] S. C. Weber, A. J. Spakowitz, and J. A. Theriot, Phys. Rev. Lett. **104**, 238102 (2010).
[99] I. Y. Wong, M. L. Gardel, D. R. Reichman, E. R. Weeks, M. T. Valentine, A. R. Bausch, and D. A. Weitz, Phys. Rev. Lett. **92**, 178101 (2004).
[100] M. P. Backlund, R. Joyner, and W. E. Moerner, Phys. Rev. E **91**, 062716 (2015).